CHALMERS
UNIVERSITY OF TECHNOLOGY

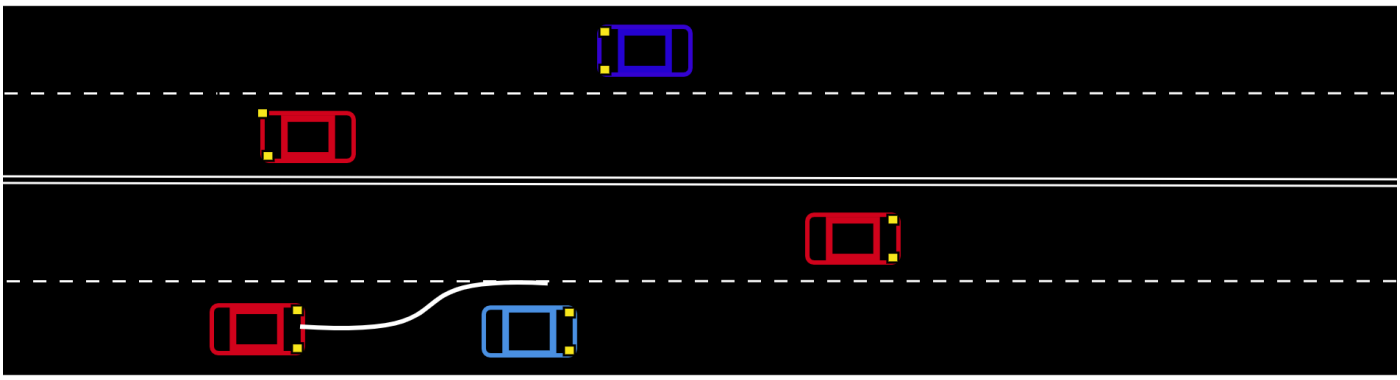

Studying the influence of trajectory and steering model choice on crash avoidance timing in simulation of rear-end conflicts that include consideration of drivers' comfortable steering potential

Master's thesis in Applied Mechanics

SHUBHAM VAIJANATH PHOOLARI

Department of Mechanics and Maritime Sciences
CHALMERS UNIVERSITY OF TECHNOLOGY
Gothenburg, Sweden 2019

MASTER'S THESIS IN APPLIED MECHANICS

Studying the influence of trajectory and steering model choice on crash avoidance timing in simulation of rear-end conflicts that include consideration of drivers' comfortable steering potential

SHUBHAM VAIJANATH PHOOLARI

Department of Mechanics and Maritime Sciences
Division of Division Name
Name of research group (if applicable)
CHALMERS UNIVERSITY OF TECHNOLOGY
Göteborg, Sweden 2019

Studying the influence of trajectory and steering model choice on crash avoidance timing in simulation of rear-end conflicts that include consideration of drivers' comfortable steering potential

SHUBHAM VAIJANATH PHOOLARI

Master's Thesis 2019:106
Department of Mechanics and Maritime Sciences
Division of Vehicle Safety
Unit of Crash Analysis and Prevention
Chalmers University of Technology
SE-412 96 Göteborg
Sweden
Telephone: + 46 (0)31-772 1000

Cover:
Visual representation of how following vehicle (red) avoids the collision with a leading vehicle (blue) following a virtual desired trajectory in a rear-end conflict.

Chalmers Reproservice / Department of Mechanics and Maritime Sciences
Göteborg, Sweden 2019-11-21

Studying the influence of trajectory and steering model choice on crash avoidance timing in simulation of rear-end conflicts that include consideration of drivers' comfortable steering potential
[Abstract]
Master's thesis in Master's Applied Mechanics
SHUBHAM VAIJANATH PHOOLARI
Department of Mechanics and Maritime Sciences
Division of Vehicle Safety
Unit of Crash Analysis and Prevention
Chalmers University of Technology

Abstract

The World Health Organization states that road crashes are expected to be the seventh leading cause of death in 2030, with road traffic injuries being the leading cause of death for children and young adults aged between 15 to 29 years of age, and the most contributing factor in road accidents is human error. Passive safety features in vehicles help depreciate serious injury to protect the vehicle occupants in a crash scenario. Some examples of this include seatbelts, crumple zones, airbags, headrests, etc. Although this has been found to be a very effective method, vehicle manufacturers are aiming to assist the driver and alleviate collisions which has resulted in an increase in the development of active safety systems which use sensors to help avoid or mitigate crashes by understanding the state of the vehicle surroundings and the driver. The modern approach to active safety from automotive industries involves building autonomous vehicles to take into account people's vulnerability to crashes and to be forgiving of common human errors. With respect to assessing active safety systems before the systems are on the market, virtual simulations are gaining momentum when compared to driving thousands of miles for evaluation of active safety functions. But this method of virtual assessment sometimes lack the knowledge of how complex a vehicle model needs to be in order to provide sufficiently accurate results. The aim of this thesis is to study the impact of trajectory and steering model choice on crash avoidance timing by taking into account the drivers' avoidance by steering in a simulation of rear-end conflicts. Three continuous steering avoidance trajectories (Virtual Desired Trajectories; VDTs), based on previous work, is used together with a single-track vehicle model with load transfer effect. A PID controller is used to track these VDTs in simulations applied to the rear-end crashes. The performance metrics in terms of collision avoidance time is evaluated for all three VDTs. Also, a sensitivity analysis is made in three parts, namely, without load transfer effect, increasing the cornering stiffness of the tires and finally by decreasing the cornering stiffness of the tires. It was observed that there were no obvious effects on the overall results in the first two simulations, but some effects were noticeable in the third simulation. The results of the three VDTs when compared, showed an observable difference.

Key words: collision avoidance, driver comfort, rear-end crashes, vehicle model, feed-back controller, highD dataset.

Contents

Preface

This study is a master thesis work carried out at Autoliv Development (industry) and at the Department of Mechanics and Maritime Sciences, Division of Vehicle Safety, Unit of Crash Analysis and Prevention, Chalmers University of Technology, Sweden (academic institution). The work was developed from January to November 2019 in the Vehicle and Traffic Safety Center at Chalmers – SAFER, in Göteborg.

Acknowledgement

First, I would like to express my gratitude to the examiner and supervisor of the project, Jonas Bärgman and Nils Lubbe, for your excellent guidance and for supporting me in any situation and how working with you was so comfortable and insightful. I would also like to thank everyone else at SAFER without whose cooperation I would not have felt the ease of working at a new work environment. A special thanks goes to Janika Heise, Mathias Lidberg, Prof. Bengt Jacobsson, Toheed Ghandriz, Alexander Rasch and Pinar Boyraz Baykas for taking the time to brainstorm with me and thus helping me in development of this work.

I am very grateful to my family and friends living overseas for supporting me throughout my journey here, for keeping me motivated and for your words of counsel. Finally, I thank all my friends, everyone I met here for always being helpful in my tough times and helped me benefit from our discussions.

Göteborg March 2019-11-21

SHUBHAM VAIJANATH PHOOLARI

Notations

Abbreviations

ACC	Adaptive Cruise Control
ADAS	Advanced Driver Assistant Systems
AEB	Automated Emergency Braking
AES	Automated Emergency Steering
AIS	Abbreviated Injury Scale
BLIS	Blindspot Information Systems
BTN	Brake Threat Number
COG	Centre Of Gravity
DAS	Driver Alert Systems
DLC	Double-Lane Change
Delta-V	Delta Velocity
ESC	Electronic Stability Control
FCW	Forward Collision Warning
FOT	Field Operational Test
FSLQ	Frequency Shaped Linear-Quadratic (Optimal Controller)
FV	Following Vehicle
GIDAS	German In-Depth Accident Study
highD	Highway Drone
HMI	Human Machine Interface
LDW	Lane Departure Warning
LPS	Last Point to Steer
LQ	Linear-Quadratic
LV	Leading Vehicle
MD	Maneuvering Distance
NDD	Naturalistic Driving Dataset
NDS	Naturalistic Driving Studies
NFOT	Naturalistic Field Operational Test
NGSIM	Next Generation Simulation
NHTSA	National Highway Traffic Safety Administration
PCM	Pre-Crash Matrix
PD	Proportional Differential
PID	Proportional Integral Derivative (Controller)
SAE	Society of Automotive Engineers
SHRP2	Strategic Highway Research Program 2
STN	Steering Threat Number
THW	Time Headway
TTB	Time To Brake
TTC	Time To Collision
TTS	Time To Steer
VDT	Virtual Desired Trajectories

Symbols

a	Slope parameter of sigmoid trajectory
a_x	Longitudinal acceleration of FV
a_y	Lateral acceleration of FV
α_f	Front slip angle
α_r	Rear slip angle
c	Point of inflection of sigmoid trajectory
c_0	Tire stiffness parameter
c_1	Tire stiffness parameter
c_w	Total axle roll stiffness
c_{fw}	Roll stiffness of front axle
c_{rw}	Roll stiffness of rear axle
C_f	Front axle cornering stiffness
C_r	Rear axle cornering stiffness
δ_f	Front steering wheel angle
δ	Steering wheel angle
h	Height of COG of FV
h_{rcf}	Front roll centre height
h_{rcr}	Rear roll centre height
Δh	Height of COG from roll axis
F_{fx}	Longitudinal force on front tire along x-direction
F_{rx}	Longitudinal force on rear tire along x-direction
F_{fy}	Lateral force on front tire along y-direction
F_{ry}	Lateral force on rear tire along y-direction
F_z	Normal load acting on tires along z-direction
g	Acceleration due to gravity
J	Vehicle inertia around z-direction
K	Understeer gradient
K_p	Proportional gain of PID controller
K_i	Integral gain of PID controller
K_d	Differential gain of PID controller
l_f	Distance of COG from front axle
l_r	Distance of COG from rear axle
L	Wheel base length
m	Total mass of the FV
MD	Maneuvering Distance
n	Steering ratio
s_{fy}	Front tire slip
s_{ry}	Rear tire slip
SG	Steering gradient
v	Velocity of the FV
v_x	Longitudinal velocity of the FV
v_y	Lateral velocity of the FV
ω_z	Yaw velocity of the FV
$\dot{v}_x$	Derivative of the longitudinal velocity of the FV
$\dot{v}_y$	Derivative of the lateral velocity of the FV
$\dot{\omega}_z$	Yaw rate of the FV

w width of the vehicle
$width_{LV}$ width of the FV
$width_{FV}$ width of the LV
x_{start} starting position of the collision avoidance maneuver
X Position of the FV along x-direction
$ypos_{FV}$ Position of the FV along y-direction from the dataset
$ypos_{LV}$ Position of the FV along the y-direction from the dataset
$y_{desired}$ Desired position of the FV along y-direction following a VDT

1. Introduction

In the context of increasing automation of vehicles, contribution of automated systems to passenger safety has gained particular interest in the last several years. Research on accidents has revealed that most incidents can be traced back to human errors [Treat et al., 1977] and end up in rear-end collisions in 28% of all police-reported traffic accidents [NHTSA, 2003]. To continuously decrease and mitigate the actual materialization of collisions, there is an ongoing work on how to develop and optimize vehicles' active and passive safety systems. While passive safety systems are constructed to mitigate the harmful outcomes during a collision, active safety systems, also called *Advanced Driver Assistance Systems* (ADAS), shall help to avoid or mitigate them before they happen [Ljung Aust, Mikael, 2012]. ADAS include various independent electronic systems which can be differentiated by four different levels of driver support [Lindgren et al., 2007]. They reach from information provision (Level 1) to warnings (Level 2) and action advice (Level 3) until independent action by the system itself (Level 4). These levels have evolved to SAE [SAEJ3016,2018] automation levels with no automation (Level 1), Driver Assistance (Level 2), Partial automation (Level 3), Conditional automation (Level 3), High Automation (Level 4) and finally Full automation (Level 5). Most ADAS variations rely on sensors installed in the vehicle, such as *Blind Spot Information Systems* (BLIS) that alerts the driver about the objects in the blind spots or *Driver Alert Systems* (DAS) provides warnings if the driver's behaviour is instable and deteriorating due to drowsiness, fatigue etc. [Lindgren,2009]. A major part of ADAS furthermore focuses on the vehicle dynamics in its specific environment and warns if a problem with the intended driving path occurs. Examples of the latter are the *Forward Collision Warning* (FCW) system measuring distance, angular position and relative speed of the car and obstacles ahead, the *Lane Departure Warning System* (LDW) that warns the drive with visual or auditory warnings if the vehicle moves away from its lane. An example of an active safety function that performs intervention rather than warning is the *Adaptive Cruise Control* (ACC) that adjusts the vehicle's speed to adapt and maintain safe distance with surrounding vehicles. The automation of those systems implies that the vehicle's system "actively selects data, transforms information, makes decisions, or controls processes" [Lee & See, 2004].

A key issue with these active safety functions, like for all other means of crash and injury prevention, is to verify if they are beneficial in traffic safety [Ljung Aust, Mikael, 2012]. [Scriven,1967] established two terms, formative and summative assessment, respectively, where formative assessment involves lab-based evaluation when the vehicle is in the development stage. The summative assessment relates to evaluation when ADAS is introduced in mass-produced cars out in the real world [Ljung Aust, Mikael, 2012]. Furthermore, in a retrospective approach [Carsten and Nilsson, 2001] the safety aspects of functional systems are studied in the early development stage, HMI (Human-Machine Interface) is validated in the mid-development stage and finally, traffic safety is validated by means of field trials. This is time-consuming and the procedure is expensive as it involves physical measurements. Thus, a prospective analysis is required to assess the effectiveness of the safety benefits of these functions introduced to the market [Alvarez et al., 2017]. Physical prospective safety evaluation includes Field Operational Tests (FOTs) of prototype systems, driving studies on simulators, closed tracks or on public roads. These procedures can together with crash

databases, provide data that can be used as information for researchers to perform virtual safety assessment through computer simulations [Bärgman, 2016]. Moreover, as concluded by [NHTSA] 94 % of the crashes in the U.S were due to human errors and deficiencies. Hence, the research focus on driver behavior in the pre-crash phase has increased through several studies over recent years to motivate safer traffic.

[Bärgman, 2016] has reflected one of the approaches to studying driver behavior in traffic and crashes as the collection and analysis of Naturalistic Driving Data (NDD). NDD allows data to be collected about the driver inconspicuously in real traffic and contains information about the vehicle, driver and driving environment. A variety of sensors like GPS, camera, radar, accelerometers, etc. are involved in the data collection process. The U.S and Europe have invested in many projects collected NDD and given researchers access to data from various sources like Naturalistic Field Operational Tests (NFOT), Naturalistic Driving Studies (NDS) and the more recent and commercially collected NDD. In NFOT, large data is collected in vehicles equipped with one or more active safety features with the focus on studying the benefits of these features and their effect on driver behavior in naturalistic conditions. Several FOT projects such as euroFOT (euroFOT,2009) and SeMiFOT (SeMiFOT,2009), have been conducted in the U.S, Japan, and European countries [Ljung Aust, 2012]. euroFOT [Benmimoun et al., 2011] is one of the first large-scale FOT data that contains data of more than 35 million kilometers around 1200 drivers. Although many problems related to ADAS's impacts on drivers can be solved through FOT studies, the issue arises when the effect of multiple ADAS functions on the driver has to be studied [Ljung Aust, 2012]. Another source of data collection from everyday driving is Naturalistic Driving Studies (NDS). Data collected from NDS does not focus on the evaluation of any specific ADAS feature and captures the naturalistic driver behavior in their everyday lives without any influence on their mindset. Whereas the data from simulators and test track do not mimic the complex traffic environments [Lewis et al., 2012] and drivers are well informed about the experiments and the purpose of data collection. There are various data collection methods in NDS which are categorized as vehicle-based and site-based. In vehicle-based collection, the data is collected from various sensors like GPS, cameras, radar, CAN, etc, inside of vehicles. These vehicle-based data facilitates understanding of individual driver's behavior, driver's action and reactions to other road users and infrastructure and driver behavior in a variety of scenarios. But the major drawback is the expensive sensors used for data collection [Bärgman, 2015]. In the U.S, the Strategic Highway Research Program (SHRP 2) is the largest and one of the most well-known vehicle-based NDS containing recordings of more than 3000 participants. SHPR2 data is only available to researchers under very controlled circumstances (see fhwa.dot.gov/goshrp2).

In site-based studies, the data is collected only in specific locations where sensors are typically is installed on the infrastructure. Site-based studies focus mostly on capturing normal driving behavior of a population of drivers extracting near-crashes or crashes, and vehicle trajectories in a specific traffic environment [Bärgman, 2015]. Next Generation SIMulation (NGSIM) dataset is a good example of a site-based dataset. It is the largest available dataset containing naturalistic vehicle trajectories used for traffic flow and driver models [Krajewski et al., 2018, B. Coifman and L. Li, 2017]. The recordings were made at four different locations covering both highway and urban scenarios. Multiple synchronized cameras were installed at top of multi-story buildings to cover the entire view at different angles. The authors in [Krajewski et al., 2018]

motivates five factors that fulfil as requirements to be suitable for scenario-based safety validation among different measurement methods.

- *Naturalistic Behavior:* Behavior of all the road users must be naturalistic
- *Static scenario Description:* The data must capture features like lane markings, speed limits, road curvature, etc.
- *Dynamic scenario Description:* The measurements cover positions and states of all road users accurately and even environmental conditions.
- *Flexibility:* Measurements should include different scenarios of traffic situations and every time of the day.
- *Effort Effectiveness:* Total effort consists of the initial effort of setting up and permanent effort of operation.

In NDS the driver is aware of the recordings and may not exhibit the real driving behavior but the other road users are unaware of the recordings being made and completely represent uninfluenced nature. Infrastructure based sensors or so-called site-based sensors or cameras can record the naturalistic behavior of the scene at a location although the drivers may be confused with these mounted cameras with law enforcement cameras thus representing atypical behavior. The static scenario descriptions derived from in-vehicle sensors are not accurate as they include localization of ego vehicle and simple information like lane markings. Infrastructure based sensors are efficient at deriving static scenarios using map data. Dynamic scenario descriptions from Naturalistic Driving Studies (NDS) are not of good quality as they measure only to a limited extent and does not include all the objects in a scene. Infrastructure sensors cover all the objects in a specific location, but the objects can be occluded if they are closer to the sensors. In comparison with respect to effort effectiveness, both NDS based data and site-based are effort effective (the total effort to set up the measurement method and effort for operation) with the main problem that the initial effort to install the sensors for site-based studies is high. With respect to flexibility, data collected in vehicle-based NDS is high as the vehicles can be driven at any weather conditions and location without any legal restrictions. Infrastructure sensors capture data in all weather conditions although typically requires permissions to be installed.

Some studies have proposed a drone-based measurement method to record road users from an aerial perspective. This approach has many strengths in terms of naturalistic behavior, static and dynamic scenario description but lacks in terms of flexibility and effort effectiveness. A new camera-equipped drone dataset from Germany is the highD (Highway Drone) dataset. The highD dataset [Krajewski et al., 2018] is a new naturalistic driving data recorded from German highways at six different locations around Cologne. The recordings were made from an aerial view in camera-equipped drones covering sections up to 420 meters of road segments in each recording that lasted for 17 minutes. Although the information on the height of the objects is lost, it can be well estimated based on the object type. The recordings from the bird-eye perspective created an advantage for the objects to be not obstructed by other objects. Using computer vision algorithms, [Krajewski et al., 2018] post-processed vehicle trajectories of 110,000 vehicles. Apart from these trajectories, predefined maneuvers were also extracted based on four categories:

- *Free Driving:* Driving without any influence from the front vehicle.
- *Vehicle Following:* Vehicle Actively following another vehicle.

- *Critical Maneuvers:* Events with Low Time to Collision (TTC) or Time Headway (THW).
- *Lane Change:* Vehicle crossing lane markings and continuing a new lane.

[Krajewski et al., 2018] used these extracted events to perform an analysis of the safety validation of highly automated vehicles. They extracted lane-change maneuvers and relevant statistics of lane change criticality. [Olleja, 2019] used these critical scenarios where vehicles with a relatively high level of decelerations were extracted among which two vehicles following each other were considered with low THW for the following vehicle (FV). Using the so-called counterfactual simulations (also called what-if simulations) the kinematics of the FV were manipulated to create crashes (removing the following vehicles braking), resulting in 86 rear-end crash events. The objective of Olljea's work was to implement an Automated Emergency Braking (AEB) algorithm as a virtual safety-assessment on crashes generated from counterfactual simulations. highD is accessible to the public unlike most other NDS datasets. The rear-end collisions generated in this data was relevant for this thesis work and as it was easily accessible, I have made use of the same.

As active safety functions are available for quite a while now, it is time-consuming to study their effectiveness when a newer active safety functions is introduced by the policy makers and companies in the market. In this case, it is necessary to introduce methods that are necessary to predict their safety benefits virtually. Counterfactual simulations (also called what-if simulations) has received increased attention to researchers for active safety evaluation [Bärgman et al, 2017]. Counterfactual simulations aim to evaluate the benefits of a safety feature in a virtual environment. It uses data from real traffic (e.g., NDS) which contains events like crashes and safety-critical events (near-crashes) [Bärgman, 2015]. This subset of NDD is used to run virtual simulations on these events by determining probable outcomes if the reality of the event was modified and validate the safety feature in a virtual environment. The difference between crashes and near-crashes is that the former is measured in terms of injury levels (e.g, Abbreviated Injury Scale (AIS), FACS, Prof. Howard R.) and it is only possible to calculate the potential severity of the crash for near-crashes. There are different methods to perform counterfactual or "what-if" simulations.

Most collision avoidance technologies and intervention systems today are tailored to rear-end collision conflicts as they constitute more than 23 % of crashes reported today [Knipling et al., 1993]. As mentioned by [Brännström et al., 2010, p.1] "the kinematics of rear-end collisions are relatively easy to predict, making threat assessment and decision making more straightforward". Considerable contributions have been made proposing state-of-the-art algorithms to avoid rear-end collisions by braking or steering autonomously. One such example is the work by [Brännström et al., 2008] who proposed a situation and threat-assessment algorithm to assist the driver to avoid the collision. The important aspect of active safety systems is that they must not disturb the normal driving tasks of the driver by false or earlier activations as this would lead to inadvertent interventions. [Brännström et al., 2008] in their work claim that their proposed method can activate interventions earlier without any noticeable false activations. In the threat-assessment part of [Brännström et al., 2008] , two threat metrics called Steer Threat Number (STN) and Break Threat Number (BTN) were calculated from the vehicle kinematics. These metrics estimates if the collision should

be avoided by steering or braking. STN is given by ratio between the required lateral acceleration to the maximum lateral acceleration while BTN is the ratio of required acceleration to the maximum acceleration by virtual braking before the host vehicle comes to rest. A similar situation assessment algorithm was proposed by [Hillenbrand et al., 2006] where the authors derive the time left for the driver to react to a rear-end conflict given the kinematics of the vehicles and the predicted model of the object. As later the driver wants to react to conflict the more is the physical constraints of vehicle dynamics exploited and based on this assumption, the authors also looked at a set of selected manoeuvres with other metrics like Time to Steer (TTS) and Time to Brake (TTB). Most automotive safety functions do not perform steering interventions today even though there often is a real-time assessment for driver avoiding the crash using steering, as a component in AEB algorithms, the steering is not actually performed. The concern in these systems is false alarming during, for example, intentional lane changes [Eidehall et al., 2007]. Also, giving complete control over the steering wheel might motivate drivers to perform secondary tasks.

Lane changes are typically extracted as sine curves, splines or polynomials [Krajewski et al., 2018; W.Yao et al., 2012]. [Schorn and Isermann, 2006] used a sigmoid equation [equation 5] to develop a collision avoiding vehicle driver assistance system with steering, braking and a combination of steering and braking. This continuous curvature is differentiable several times. [Schorn and Isermann, 2006] use this equation as the desired trajectory to guide the vehicle on the desired trajectory using a feed-back Proportional Differential (PD) type controller. They also used the Local linear controller approach [Nelles,2001] to build a network of controllers for different velocities. [Pongsathom et al., 2019] proposes a hyperbolic tangent curve [equation 6], used to perform a double-lane change (DLC) maneuver in a closed-loop test. This curve was incorporated as the desired path where a driver model was used to follow this path using a lane tracking control law. [Xiangkun He et al.,2018] uses a fifth-order polynomial [equation 7] as a collision-free trajectory to develop an autonomous vehicle for collision avoidance. This equation has been widely used in lane-change experiments and trajectory planning for autonomous vehicles. [Xiangkun He et al.,2018] propose a backstepping sliding mode controller to track this path during emergency steering. The controller used is made robust enough to handle non-linear cornering response of tires and external disturbances to the vehicle. Furthermore, [Masayoshi Tomizuka,1994] used three types of controllers, including linear-quadratic (LQ) optimal controller, frequency shaped linear-quadratic optimal controller (FSLQ) and sliding mode controller, tested on different types of lane-change trajectories termed as 'Virtual Desired Trajectories (VDT)'. [Masayoshi Tomizuka,1994] found that the sliding mode controller was superior in closed-loop tracking of the desired trajectory.

Driver comfort is an important aspect to be considered while developing these lane change trajectories. As Bekiaris et al. (1997) stated, "people are generally reluctant to release control of their car but are willing to do it in emergency situations". The negative perception from the driver usually results from his mistrust in the system which is triggered by unreliable or mistimed measures [Parasuraman & Riley, 1997; Bliss & Acton, 2003]. As this mistrust can become a barrier to technology adoption [Bellem, p.27], both the system algorithm and driver interface of ADAS should be optimized with regards to the driver's specific "conditions, limitations, and preferences." [Lee et al., 2004]. The ultimate goal of ADAS is hence "to create a traffic environment where the driver never exits the comfort zone while at the same time the comfort zone is always kept within the safety zone boundary." [Lindgren, 2009] A challenge of defining

such a comfort zone, however, is that comfort is a highly subjective perception. Furthermore, the perception of parameters like lateral acceleration and headway distance is situational, as it changes with increasing velocity for instance. [Bellem, Hanna,et al., 2018]. In the past, extensive research has been done to investigate driver's comfort perceptions and define a common understanding of its standards in the context of automated systems. In her dissertation on comfort-related driving style preferences in automated driving, Hanna Bellem investigated participants' perception of driving styles both in manual and simulated automated execution. In the first step, she let participants test three different driving styles, which are *normal everyday driving, comfortable driving,* and *dynamic driving,* on both rural and urban streets and highways. Based on the participants' ratings, Bellem concluded that *maximal acceleration* was the best predictor of driving comfort. Moreover, less acceleration, as well as smoothness of scenarios and anticipatory actions were found to be favorable. Secondly, Bellem set up a simulator study to let participants rate different automated driving configurations in driving on highways-scenarios. As expected, "symmetrical acceleration and thus variation with the smallest overall jerk was preferred" [Bellem, p.81]

[Bae et al. 2015] give a more detailed explanation about how lateral acceleration is related to drivers' comfort. They state that the major cause for perceived discomfort is a temporal motion sickness from excessive acceleration or jerks. The lateral acceleration depends on the speed of cornering or lane changes and the ranges of the corner [Bae et al., p.2] which explains the need for moderate maneuvers to make passengers feel comfortable. With this conclusion, the question arises which maximum acceleration value is generally acceptable for the construction of ADAS. Hugemann and Nicke (2003) published a broadly-cited study on lateral accelerations in normal daily driving. For a radius of 20 to 40 meters, their test drivers indicated a preference for 5.3m/s^2 as maximum lateral acceleration, i.e. the 90th quantile. Multiple other studies have relied on same or at least similar reference values for lateral acceleration. In their experimental study autonomous driving style simulations, [Karjanto et al., 2017] investigate ranges of accelerations with regards to driving experience and acceptance and rely on Hugemann and Nicke's 5.30 m/s^2 or 0.54 g as upper limit in a human-driven car. Based on his investigated data on driver preferences, [Levison et al.,2017] recommends a lateral acceleration of 0.4 g for speed decisions in passenger cars. Brännström et al. identified physical driver limits as thresholds that were not exceeded by typical drivers during normal driving. This thesis work consequently selected 5 m/s^2 as maximum lateral acceleration as driver comfort limit.

1.1 Aim and main hypotheses

The aim of this thesis is to study the impact of trajectory and steering model choice on crash avoidance timing when simulating the application of a safety system that include drivers' avoidance by steering within comfortable limits, for rear-end conflicts. The goal is to use three continuous curvatures termed as “Virtual Desired Trajectories (VDTs)” on rear-end crashes from highD through virtual simulations and at the “Last Point to Steer (LPS)” the driver can steer and avoid the collision within the set comfort limits . At this point, performance metrics like Time-to-Steer (TTS), Time-to-collision (TTC) and other metrics are derived for each of the proposed VDT. The three VDTs are used as inputs to a one-track vehicle lateral dynamics model and a feed-back controller is used to track the desired trajectories to perform the evasive maneuver. The simulation environment implemented in Matlab performs the tasks of decision-making, path-following control, and collision avoidance assessment in real-time on highD crash data. The final goal is to perform a sensitivity analysis by modifying the parameters in vehicle model to test their sensitivity on the collision avoidance timing.

Base on this aim the following hypotheses were established as a start point of the thesis work:

- If the lateral and longitudinal load transfer corrections are excluded in the lateral dynamics vehicle model, the threat avoidance timing (TTS) will decrease.
- With an increase in cornering stiffness of the vehicle tires, the vehicle tends to be understeered. This decreases the TTS because the required steering angle is less and hence causes the vehicle to reach the equilibrium early with the action of the feedback controller on the steering wheel.
- Among the three VDTs used in this thesis, the hyperbolic tangent VDT has larger derivatives and this results in the higher values of TTS. The sigmoid VDT used has much lower derivatives and results in the lower TTS values while the fifth-order polynomial used falls in between hyperbolic tangent and the sigmoid.

2. Method

This section provides a detailed description of the method implemented throughout the thesis work. Section [2.1] describes calculations made on relevant parameter from the highD data set used in this thesis. Section [2.2] explains the different manoeuvre profiles used in previous studies and their relevant design parameters. In section [2.3], the single-track vehicle lateral dynamics model with load transfer effect used for motion of the FV is described. Section [2.4] describes how the different VDTs are integrated into the vehicle model using a feed-back controller that is described in the Section [2.5]. Section [2.6] explains the method used for implementation in simulations to find the last point to steer for the driver within comfort limits. Finally, section 2.7 explains the overall process of collision avoidance assessment on rear end crashes in highD.

2.1 Calculations from highD

As previously mentioned, this study used dataset of crashes based on the highD naturalistic driving dataset, containing rear-end collision scenarios that were used for evaluation of AEB algorithm assessment by [Olleja,2019]. For collision avoidance assessment to be applied to this crash dataset, it is required to compute the lateral distance that the following vehicle (FV) would need to move to avoid the collision with the lead vehicle (LV) in each time step. This lateral distance is called 'offset' throughout this thesis work and is assumed to be the distance that the following vehicle needs to cover to avoid the collision within the driver's comfort limitation [Hugemann & Nicke, 2003].

The first step of this thesis work began by aaccessing the real-time coordinates of both the following and the lead vehicle from the highD crash dataset from each crash event. Figure [1] and Figure [2] give visual representations of the geometrical calculation made to get the left and right lateral offset based on the FV's relative position to the LV, that is, in each time step if the FV is at the left or right of LV's centre. These offsets values were later used as one of the design parameters to the VDTs.

If $ypos_{FV} > ypos_{LV}$, this means that the following vehicle is on the left side of the lead vehicle as shown in Fig 1;

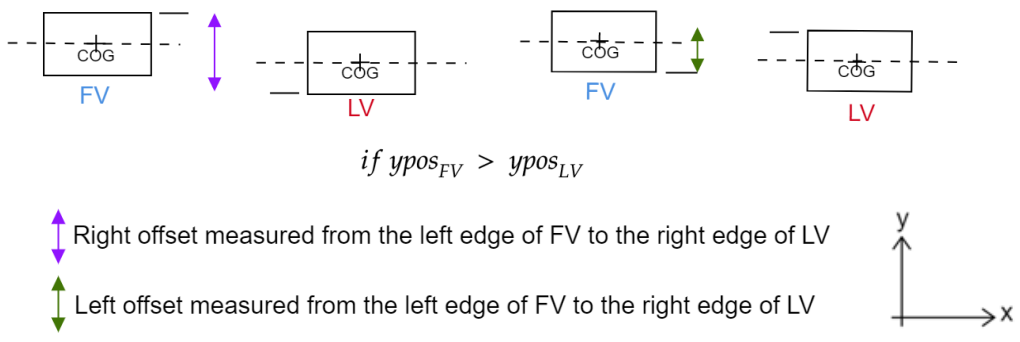

Figure 1 *Calculation of right and left lateral offset when FV is at the left side with respect to the LV*

$$RightLateralOffset = \frac{width_{LV}}{2} + \frac{width_{FV}}{2} + abs(ypos_{LV} - ypos_{FV}) \quad (1)$$

$$LeftLateralOffset = \frac{width_{LV}}{2} + \frac{width_{FV}}{2} - abs(ypos_{LV} - ypos_{FV}) \quad (2)$$

If $ypos_{FV} < ypos_{LV}$, this means that the following vehicle is at the right side of the lead vehicle as shown in Fig 2;

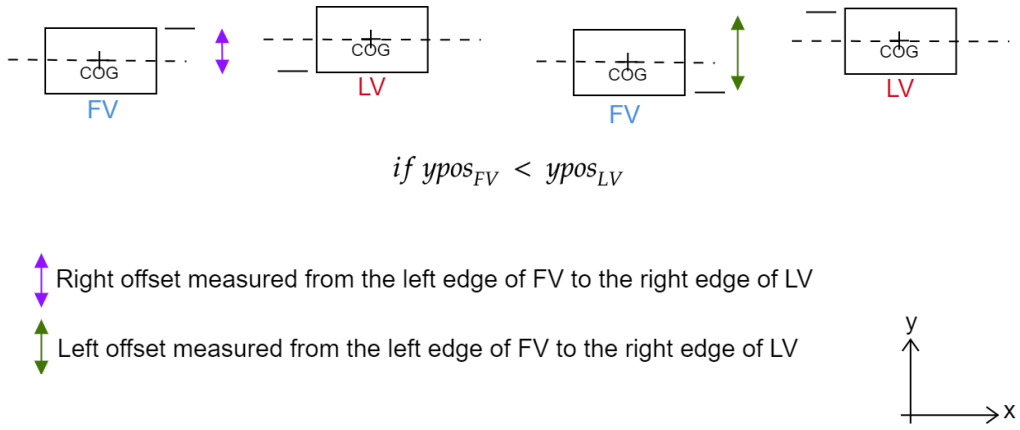

Figure 2 *Calculation of right and left lateral offset when FV is at the right side with respect to the LV*

$$RightLateralOffset = \frac{width_{LV}}{2} + \frac{width_{FV}}{2} - abs(ypos_{LV} - ypos_{FV}) \quad (3)$$

$$LeftLateralOffset = \frac{width_{LV}}{2} + \frac{width_{FV}}{2} + abs(ypos_{LV} - ypos_{FV}) \quad (4)$$

where $\boldsymbol{width_{LV}}$ is the width of the LV and $\boldsymbol{width_{FV}}$ is the width of the FV.

2.2 Virtual Desired Trajectories (VDT)

As the objective of the thesis work is to propose three continuous curvatures, the VDT candidates were selected based on the literature review from previous work [see section 1]. The input parameters to these trajectories are generalized to the velocity of the FV with lateral acceleration as a constraint. In their work on threat assessment algorithm, [Hugemann & Nicke, 2003] suggests 5 m/s^2 as driver comfort limit which was used as reference in this thesis work.

Furthermore, each trajectory has its own design parameters that produce a continuous curvature in a closed-form expression. The criteria to compare the VDTs is to evaluate the time required for the FV to laterally moving along the curve with respect to LV to avoid the collision by steering. This time is referred to as 'Time-to-Steer' (TTS) throughout this thesis work. The evaluation of other performance metrics is discussed in section [2.7]. For a given velocity and offset, figure [3] shows the design parameters of each trajectory.

- *Sigmoidal trajectory*
  The sigmoid trajectory from [Schorn and Isermann, 2006] is given by,

$$y_{desired} = \frac{offset}{1 + e^{(-a \cdot (X - x_{start} - c))}} \tag{5}$$

Here, '*a'* is the slope parameter and *'c'* is the point of inflection in the middle of the path.

- *Hyperbolic Tangent trajectory*

  The equation used by [Pongsathom et al., 2019] for their double-lane change experiment is given by,

$$y_{desired} = \left(\frac{offset}{2}\right) \cdot \left[1 + tanh\left\{\frac{2}{MD} \cdot pi \cdot \left(X - x_{start} - \frac{MD}{2}\right)\right\}\right] \tag{6}$$

- *Fifth-Order cubic polynomial*

  The fifth-order polynomial from Xiangkun He's work is given by,

$$y_{desired} = offset \cdot \left[10 \cdot \left(\frac{X}{MD}\right)^3 - 15 \cdot \left(\frac{X}{MD}\right)^4 + 6 \cdot \left(\frac{X}{MD}\right)^5\right] \tag{7}$$

where X is the x-coordinates, x_{start} is the current position in x-direction where the vehicle initiates collision avoidance and MD is the maneuvering distance, that is, the distance between the start point of the maneuver to the endpoint of the maneuver. Note that MD will be used extensively when describing the results. Figure [3] shows the visual representation of the above three VDTs and their design parameters in the cartesian coordinate system for the same velocity ,offset and MD for all three VDTs.

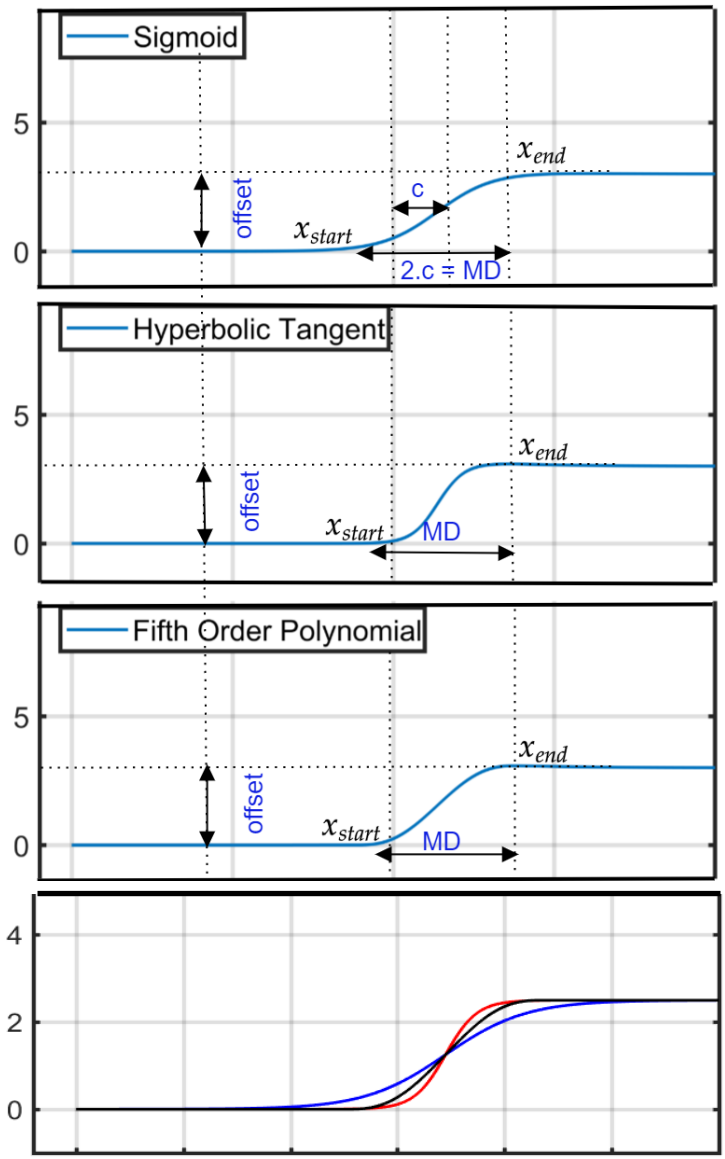

Figure 3 *Sigmoid, hyperbolic tangent and Fifth-order polynomial trajectories for the same Maneuver Distance (MD), Velocity and offset. The last plot shows hyperbolic tangent (red), sigmoid (blue) and fifth-order polynomial (black) for the same MD.*

2.3 Vehicle Model for Lateral Dynamics

This section motivates the complete modelling used for the motion of the FV and describes its lateral dynamics. The model used is of type one-track which facilitates lateral and longitudinal load-transfer correction. The mathematical model was implemented in Simulink blocks to perform further simulations for the collision avoidance assessment using steering.

- The model is a single-track vehicle model with 3 degrees of freedom with lateral and longitudinal load transfer with combined slip calculations which makes it an enhanced single-track model.
- The motion of the vehicle is assumed to be on a flat road with no aerodynamic drag and rolling resistance being considered.
- The equations are motivated for transient state with steady roll and pitch.

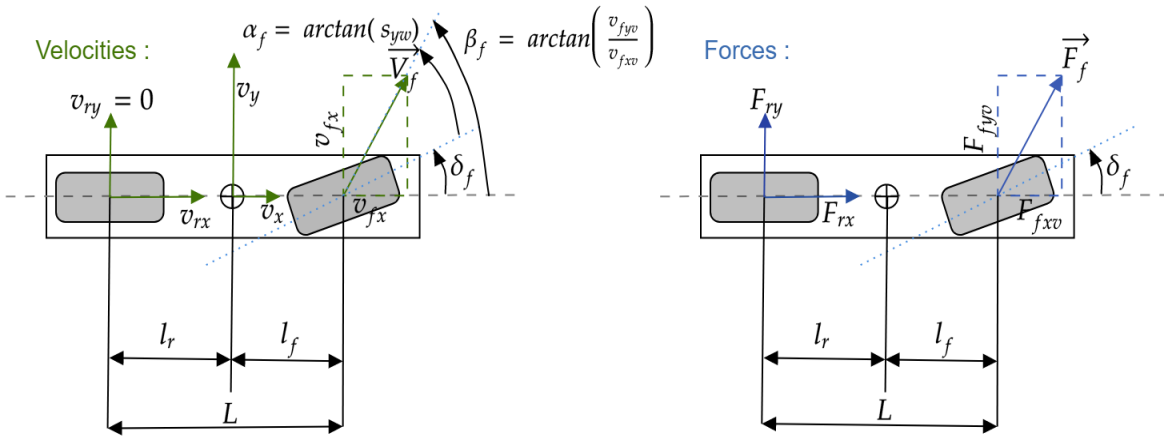

Figure 4 One-track Lateral Dynamics Model

2.3.1 Chassis

The equations of motion for the above single-track model are given by,

$$\dot{v_x} = \frac{(F_{fx}.\cos(\delta_f) - F_{fy}.\sin(\delta_f)) + F_{rx}}{m} + \omega_z * v_y \qquad (8)$$

$$\dot{v_y} = \frac{\left(F_{fy}.\cos(\delta_f) + F_{fx}.\sin(\delta_f)\right) + F_{ry}}{m} + \omega_z * v_x \quad (9)$$

$$\dot{\omega_z} = \frac{\left((F_{fy}.\cos(\delta_f) + F_{fx}.\sin(\delta_f)) * l_f - (F_{ry}.l_r)\right)}{J} \quad (10)$$

where $\dot{V_x}, \dot{V_y}\ and\ \dot{\omega_z}$ are the first derivates of longitudinal velocity (v_x), lateral velocity (v_y) and yaw velocity (ω_z) respectively. The terms $F_{fx}\ and\ F_{fy}$ are the longitudinal and lateral forces of the front wheel respectively. These force components for the front wheel are motivated in terms of vehicle's front wheel coordinates as the model is front wheel steering. 'l_r' is the distance from the centre of gravity to rear axle and 'l_f' is the distance from the centre of gravity to the front axle. J is the moment of inertia of the vehicle model along the Z-axis.

2.3.2 Tire Model

The tire model is designed by first setting up the equations of the forces that influence the tires and the axles during cornering. Firstly, the forces acting on each tire are established to further consider the combined slip effects acting on each tire.

The longitudinal forces acting on both front and rear tires respectively are given by,

$$F_{fx} = F_{rx} = \mu \cdot F_z = 0\ (\ no\ braking\ included) \quad (11)$$

where μ is the road friction coefficient which was assumed to be 0.8 and F_z are the vertical loads acting on each front and rear axle respectively and in the static condition, is estimated as,

$$F_z = \frac{m \cdot g}{2 \cdot L} \cdot [l_r; l_r; l_f; l_f] \quad (12)$$

where l_r is the distance from the centre of gravity to rear axle and l_f is the distance from the center of gravity to the front axle; L is the wheelbase length.

The slip effect is a phenomenon that occurs due to relative motion between the road and the tire surface. The influence of slip occurs when the vertical loads acting on the tire is greater than zero as the vehicle is in motion. When the total sum of the torque on both the propulsion shaft and the wheel reaches a significant level, the tire deforms due

to its material characteristics. This deformation, in turn, introduces longitudinal forces in the tire and creates a difference in the speed between the surface speed of the wheel compared to the speed between axle and road surface. The slip effect also has its lateral counterpart when the tires are inclined at an angle. During cornering, the lateral component of the velocity is introduced in the tire and the angle between the longitudinal direction and the lateral is termed as 'lateral or side slip'.

Both longitudinal and lateral components of slip are computed as follows.

Front tire slip (s_{fy}) is,

$$s_{fy} = \frac{(v_y + l_f.\omega_z) \cdot \cos\delta - (v_x \cdot \sin\delta)}{|(v_y + l_f.\omega_z) \cdot \sin\delta + (v_x \cdot \cos\delta)|} \tag{13}$$

Rear tire slip (s_{ry}) is,

$$s_{ry} = \frac{v_y - l_r \cdot \omega_z}{|v_x|} \tag{14}$$

where v_y is lateral velocity, v_x is the longitudinal velocity, and ω_z is the yaw velocity.

The front axle stiffness (C_f) for both front wheels are combined and established,

$$C_f = 2 \cdot \left(c_0.F_{fz} + c1.F_{fz}^2\right) \tag{15}$$

Similarly, the rear axle stiffness (C_r) for rear wheels is given by,

$$C_r = 2 \cdot \left(c_0.F_{rz} + c_1.F_{rz}^2\right) \tag{16}$$

where c_0 and c_1 are tire stiffness parameters. Finally, the constitutive relations can be written as a linear relationship between the lateral forces and lateral slip as,

$$F_{fy} = -C_f \cdot s_{fy}, \; F_{fy} = -C_r \cdot s_{ry} \tag{17}$$

2.3.3 Load Transfer

During steady state cornering, the vehicle experiences a centrifugal force at its Centre of Gravity (COG) against the direction of lateral acceleration. This causes the vehicle body (sprung mass) to roll around an axis called roll axis. This roll axis is a line passing through two points called roll centres which are usually placed below COG level. As a consequence of the body roll , load transfer takes place between the right and the left wheels which affects the lateral forces and increases the normal loads on one side of the vehicle body. The variation of lateral forces (F_y) and normal loads (F_z) can be represented as a saturation curve [Bengt Jacobsson et al., 2017]. Increase in load transfer reduces lateral forces and also cornering stiffnesses of the front and the rear wheels.

Since the tire loads need to be redistributed, the following load transfer equations are used. For the longitudinal load transfer assumptions are that the vehicle runs on a flat road without any aerodynamic drag and for lateral load transfer, the assumption is to have a non-rigid suspension with different roll stiffness in the front and rear. Both tires of the front and rear axles need to be considered hence the load transfer is calculated for all the wheels individually to determine the individual tire stiffness. This tire stiffness is then combined to form the axle stiffness as given equations [15 & 16] above.

Longitudinal load transfer equations for front left and right wheels are given by,

$$\Delta F_{fzleft_{long}} = \Delta F_{fzright_{long}} = -\frac{m \cdot a_x \cdot h}{2 * L} \tag{18}$$

Longitudinal load transfer equations for rear left and right wheels are given by,

$$\Delta F_{rzleft_{long}} = \Delta F_{rzright_{long}} = \frac{m \cdot a_x \cdot h}{2 \cdot L} \tag{19}$$

Lateral load transfer for front left wheel,

$$\Delta F_{fz_{lat}} = -(m \cdot a_y) \cdot \left(\frac{h_{rcf} \cdot l_r}{L \cdot w} + \frac{\Delta h \cdot c_{fw}}{w \cdot c_w}\right) \tag{20}$$

Lateral load transfer for front right wheel,

$$\Delta F_{fz_{lat}} = (m * a_y) * \left(\frac{h_{rcf} \cdot l_r}{L \cdot w} + \frac{\Delta h \cdot c_{fw}}{w \cdot c_w}\right) \tag{21}$$

Lateral load transfer for rear left wheel,

$$\Delta F_{rz_{lat}} = -(m \cdot a_y) \cdot \left(\frac{h_{rcr} . l_f}{L \cdot w} + \frac{\Delta h \cdot c_{rw}}{w \cdot c_w}\right) \tag{22}$$

Lateral load transfer for rear right wheel,

$$\Delta F_{rz_{lat}} = (m \cdot a_y) \cdot \left(\frac{h_{rcr} \cdot l_f}{L \cdot w} + \frac{\Delta h \cdot c_{rw}}{w \cdot c_w} \right) \tag{23}$$

where m is the mass of the vehicle and a_x and a_y are the longitudinal and lateral accelerations respectively measured in m/s^2. w is the width of the vehicle. The terms h_{rcf} and h_{rcr} are the roll center heights with respect to the front and rear axles in meters respectively. c_{fw} and c_{rw} are the roll stiffness for the front and rear axles respectively measured in $\frac{N-m}{rad}$. Δh is the height of COG from the roll axis.

2.4 Path Following Control

In situations when the collision cannot be avoided by emergency braking, modern driver assistance systems plans interventions using lateral control systems. The control systems receive input variables from sensors to plan an evasive trajectory in real-time and follow that trajectory using feedback control. Based on the above literature analysis on successful research achievements, a more straightforward approach as in [Schorn and Isermann, 2006] was employed in this thesis work. Firstly, a feed-forward control law with a self-steer gradient was defined [equation 24]. It considers wheelbase length, the velocity of the vehicle, and curvature of the VDT. This understeer gradient is mostly 'positive' which means that most vehicles require higher steering angle input for a given curve [Bengt Jacobson et al.,2017] as the speed increases. The same control law was set-up for all the VDTs defined in section [2.2] for simulations. Feed-back control is also considered in the implementation as feedforward alone does not yield the desired results due to system dynamics being neglected. For this, a simple PD type controller was used in the feedback to control the deviation between the VDT and the output.

Figure [5] represents the model of the control structure that was developed in Simulink. The feed-forward control law is written as,

$$\delta_{FF} = n \cdot (L + SG \cdot v^2) \cdot \kappa \tag{24}$$

Where, κ = 1/R is the curvature of the VDT expressed in m^{-1} and 'n' is the steering ratio. As all the VDTs used in this thesis work were differentiable up to order 2 and expressed in cartesian coordinates, the radius of the curvature is calculated using the following equation.

$$R = \left| \frac{(1 + y')^{3/2}}{y''} \right| \tag{25}$$

As the feedforward loop ends, the deviation $e = |y_d - y_s|$ between the output and the VDT is fed as feedback control δ_{FB}. The steering wheel is finally controlled by the combined effect from feedforward δ_{FF} and feedback signals (δ_{FB}).

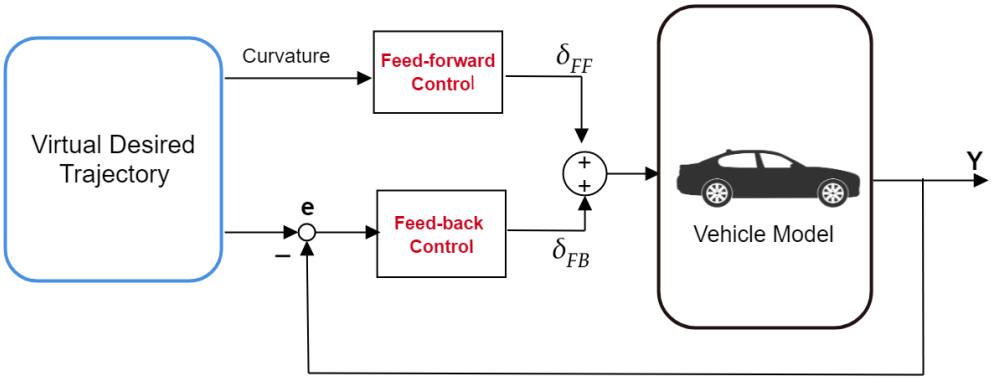

Figure 5 *Path following control structure with combined feedforward and feedback control*

2.5 PID controller

PID controllers are widely used controllers for a wide range of industrial applications as they are simple, effective and easy to implement [K.E. Arzén, 1999]. Although the modern controllers are complex and the structures of the controllers are more elaborated, PID has proved to be a potent controller when the goal is to track a specified path especially in autonomous vehicles and robotic vehicles [Montemerlo, M. et al., 2006]. In this thesis work, it is used as a feedback control and consists of a **P**roportional, **I**ntegral and **D**erivative (PID)action. Its functionality is based on the error between the reference signal and the measured output to minimize them over time. In this case, the objective is to minimize the cross-track error between the VDT and the output [e = min $|y_d(s)-y(s)|$] from the plant model.

A block representation of the PID controller is depicted in Figure [5]. Equation [26] shows the mathematical representation of parallel form in terms of cross-track error (e), the terms K_p ,K_i and K_d are the proportional ,integral and derivative gains respectively.

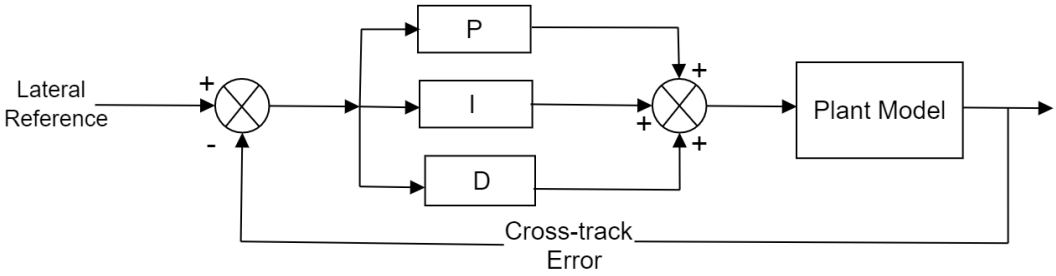

Figure 5 Structure of the PD controller

The gains K_p and K_d determine the characteristics of the output performance and it is necessary to tune these gains with regards to suitable and reliable tuning methods. Ziegler-Nichols method [Julio E. Normey-Rico,2001] for tuning is the most commonly robust used tuning process for PID controllers. This tuning process was not required in this control problem as there was an automatic tuning option available in Simulink. The PID autotuner by default linearizes the plant model and based on the estimated measured data from the plant model, it lets the user interactively adjust the frequency response to reach the target frequency response and bandwidth. This, in turn, controls gain values typically leading to a reasonably robust PID and better performance of the output.

Different compositions of the PID gains were required to solve this control problem for different range of velocities and offsets. Hence, the first step of the tuning process began with Kp, Ki and Kd set to [1,1,1] for a velocity of 30 m/s and offset value of 1m. Next, using the autotuner option in Simulink, the cross-track error between the output and the VDT was reduced. The updated gain values were tested for different velocities more than and less than 30 m/s and offsets to check if the performance was similar for a certain velocity range. The process was repeated to obtain the gain values for different speed ranges to be used for final simulations. Table [1] shows the PID gain values used for the simulations for different velocity ranges. These values were applicable to all the proposed VDTs.

Furthermore, a low-pass filter was included in the feedback control to eliminate the disturbances in the steering wheel performance as this would practically affect driver and passenger comfort. Figure [5] shows the simulation results from the path-following control without the filter while Figure [6] shows how the high-frequency disturbances were damped to produce a smooth output using a low-pass filter.

$$u(t) = K_p \cdot e(t) + K_i \cdot \int_0^t e(t)dt + K_d \cdot \frac{de(t)}{dt} \tag{26}$$

Velocity Range (m/s)	K_p	K_i	K_d
>30 - 37	100.6426	0	60.0961
>25-29	50.6426	0.1221	100.0961
>16-25	50.88019	0.1221	80.7475

Table 1 PID gain values for the different velocity range

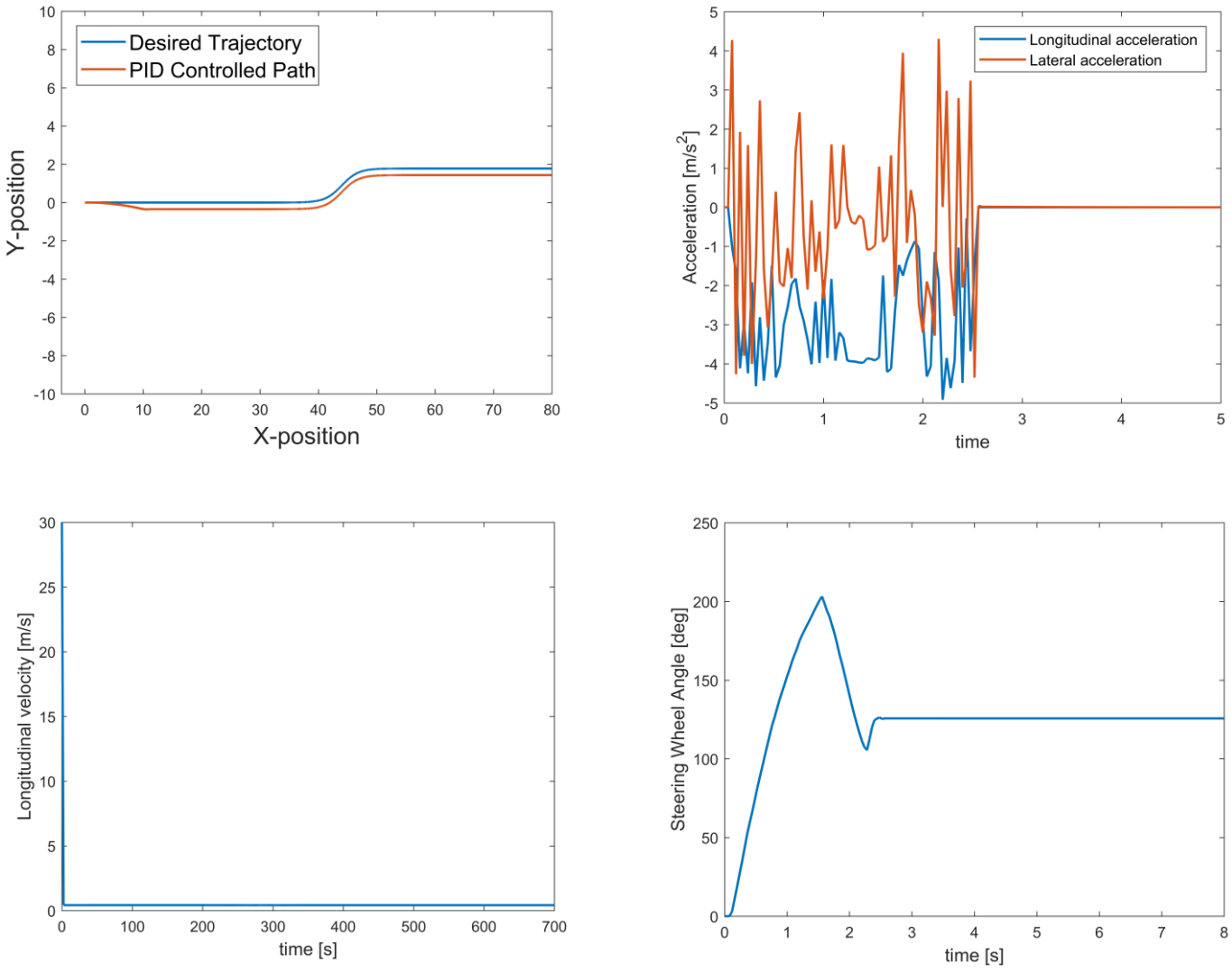

Figure 6 Results from the path-following control without the filter

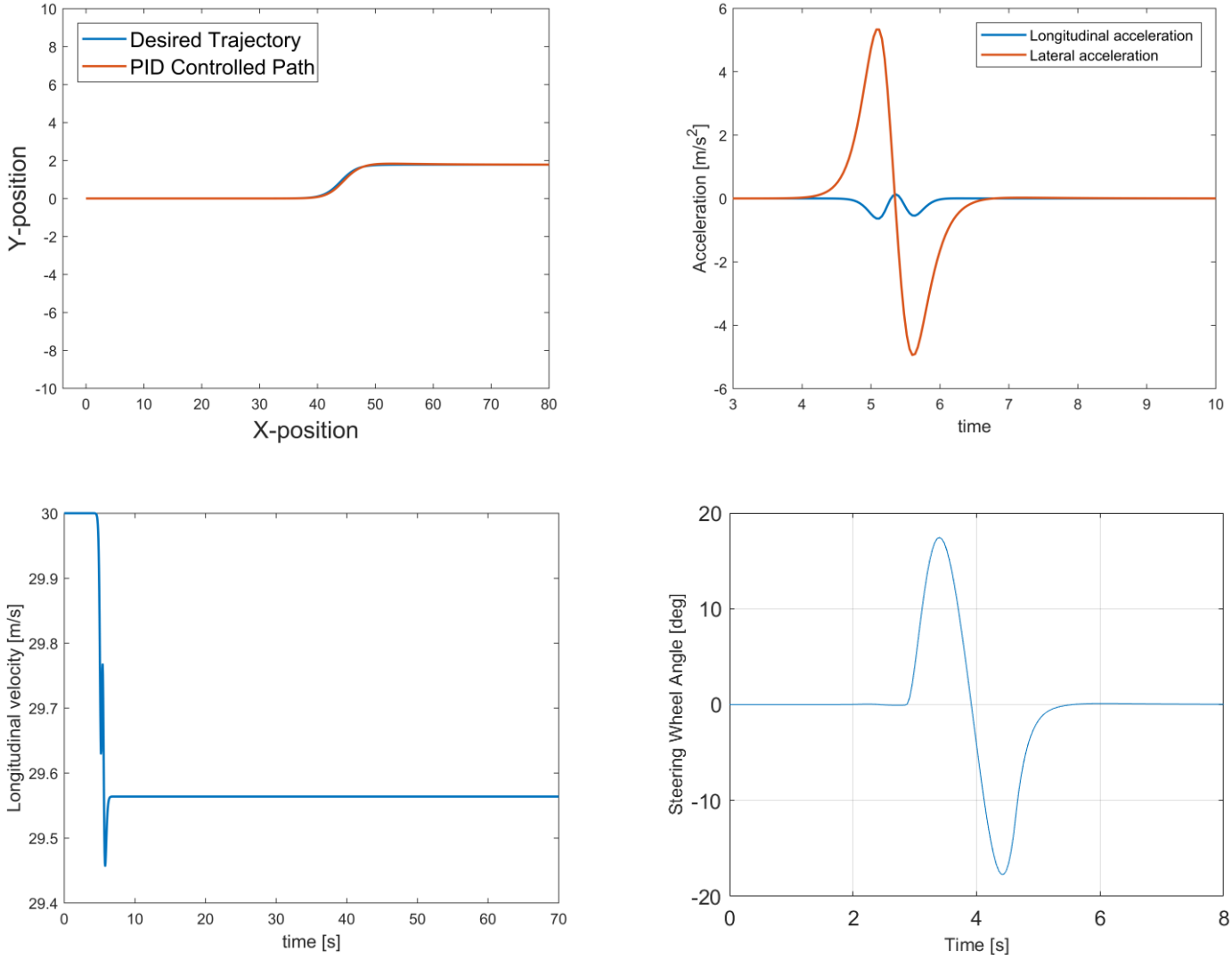

Figure 7 Results from the path-following control using the filter

2.6 Identification of the Last Point to Steer (LPS)

As previously mentioned, this one of the goals is to evaluate three continuous curvatures implied as VDTs in terms of their performance metrics applied to rear-end crashes. To obtain these performance metrics, the FV driver's ability to avoid the collision with the LV within the comfort threshold first needs to be assessed. When these VDTs are subject to the constraint of driver comfort, the design parameter MD has to be identified for a given velocity and offset. For this, the simulations are made for the FV to move along the VDT at each time step. Based on the algorithm discussed in this section, the value of MD defines the harshest maneuver at each step that is close to the lower bound of driver comfort lateral acceleration. Finally, an assessment on

collision detection is made, that is, if at any time '*t'* the FV collides with the LV, the previous time step *'t-1'* is considered as the latest point to steer [Brännström, M.,2014] at which the driver needs to initiate steering to avoid the collision.

Firstly, it is obvious that in all the proposed VDTs, the dependent variable MD impacts the lateral acceleration and TTS significantly, for a given velocity and offset. That is, the shorter the MD, the quicker is the maneuver and the higher is the lateral acceleration. Also, a shorter MD could also support intervention systems to automatically steer as late as possible when the driver is no longer capable of avoiding the conflict. However, the functionality of the automatic steering is not part of the contribution in this thesis work. This minimization task of MD was formulated mathematically as a continuous function with applied constraint of driver comfort lateral acceleration leading to equation [28].

The Newton-Bisection method [Ehiwario, J.C.,2014] was chosen as an optimization algorithm to find the LPS with respect to all the VDTs. Typically, the Newton-Bisection method is used as a root-finding method on continuous functions that have known roots with opposite signs. It continuously bisects the interval with these known roots creating subintervals converging to a final root.

Although slow, this method is robust and simple and well suited to be part of the defined problem statement discussed in the section. The lateral acceleration is a function of MD and can be represented as,

$$a_y = g(MD) \tag{27}$$

Since the value of MD at which the lateral acceleration will be closest to driver comfort lateral acceleration ($a_{y\_drivercomfort}$) needs to be found, the continuous function used for bisection becomes,

$$f(x) = g(MD) - a_{y_drivercomfort} \tag{28}$$

The driver comfort limit was set as 5 m/s^2 , the above function becomes

$$f(x) = g(MD) - 5 \tag{29}$$

where $g(MD)$ is the output lateral acceleration for one of the VDTs implemented in Simulink model. It was found that the interval [1,35] meters for MD satisfy the conditions for $f(x)$ to have opposite signs for all the speeds of the FV in the given dataset. Moreover, it was also tested to work for different offset ranges. This is represented by the figure [8] where the continuous function has its two roots [a,b] at the extremes.

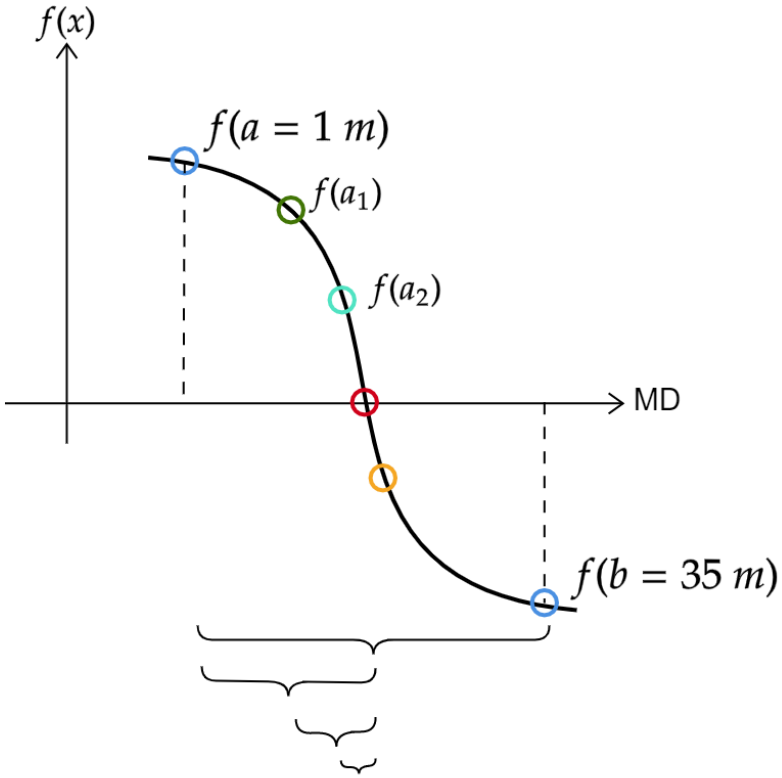

Figure 8 *An illustration of the bisection process. The red dot is the root of the continuous function*

Furthermore, the iteration tasks of the bisection follow these steps :

1. Compute the midpoint of the interval [a,b] $c = \frac{a+b}{2}$
2. Calculate the function $f(c)$ at this midpoint
3. Examine to check what part of the interval c belongs to

   i.e. if $f(a) \cdot f(c) < 0$
   c = b and the new interval is [a,c] else if $f(a) \cdot f(c) > 0$, then c=a and the new interval will be [c,b].
4. Compute the lateral acceleration for the midpoint *'c'*.
5. Check if the lateral acceleration for this midpoint is close to 5 m/s^2 by comparing with a set tolerance of 0.1 m/s^2 as convergence criteria.
6. If the convergence check in previous step fails, repeat step 1 to bisect the new interval interval for a new midpoint.
7. Repeat step 5 to check the convergence of lateral acceleration for this new midpoint.
8. If the convergence is satisfied, stop the iteration else repeat the bisection.
9. The final value of the MD results in a harshest maneuver whose lateral acceleration is close to 5 m/s^2.

2.7 Collision Avoidance Assessment

This section describes how the virtual simulations are made on highD crashes and relevant performance metrics are extracted. The algorithm is divided into several problems with each problem forming one step of virtual simulation in a Matlab script that performs one of the tasks of decision making, threat assessment or control of the vehicle. Figure [9] shows the visual representation of the framework of how the simulations perform the real-time driver collision avoidance assessment inclusive of datasets and vehicle models.

To begin with, to perform evasive maneuve by steering, the Simulink model needs access to the following parameters to run the simulations in every time step:

- The velocity of the following vehicle
- Right and Left Offset
- X-positions of FV which is the start point of maneuver
- Length and Width of FV
- PD gain values (K_p and K_d)

From this point on, the process of driver collision avoidance assessment follows these steps:

1. *Decision Making:* After the highD crash data is imported, the initial step for the FV to decide is to turn left or right. Based on the offset calculations discussed in section [1.1], the FV selects the minimum value of offset among the left or right offset.

2. *Identification of Latest point to Steer:* When the decision on the left or right turn is made by the FV, the FV needs to move laterally to reach that offset following curvatures defined by the VDTs. When the FV has accessed the respective design parameters for each of the VDTs and those mentioned above, the analysis is made on the Maneuver Distance (MD). Consequently, an optimal value of MD is obtained for all three cases that result in a maneuver that is close to the driver's comfort limit.

3. *Path Control:* As the motion of the vehicle is characterized by the optimal MD in the previous step, the next step for the FV is to perform the evasive maneuver starting at time 't_i'. The PID controller acquires the gain values based on the velocity at that time step and controls the steering wheel to follow the path defined by the VDTs.

4. *Collision detection:* As both FV and LV are changing their [X,Y] positions at discrete times, it is necessary to check if the FV collided with the rear end of the LV at each time step. Figure [9] illustrates the process of collision detection in a prediction space by considering the movements of both vehicles in real-time. The sample time for both vehicles used was 0.04s. First, both FV and LV are modelled as rectangles defined by their length and width. Next, the positions of the front right corner and the front left corner of the FV is computed as,

$$X_{cornerfr} = X_{pos} + \frac{Length_{FV}}{2}, Y_{cornerfr} = Y_{pos} - \frac{width_{FV}}{2} \quad (30)$$

$$X_{cornerfl} = X_{pos} + \frac{Length_{FV}}{2}, Y_{cornerfl} = Y_{pos} + \frac{width_{FV}}{2} \quad (31)$$

where $X_{cornerfr}$ and $X_{cornerfl}$ are the X-positions of the front right corner and front left corner of the FV respectively while $Y_{cornerfr}$ and $Y_{cornerfl}$ are the Y-positions of the front right corner and the front left corner of the FV respectively.

Similarly, the positions of the rear left corner and the rear right corner of the LV are computed as,

$$X_{cornerrl} = X_{pos} - \frac{Length_{LV}}{2}, Y_{cornerrl} = Y_{pos} + \frac{width_{LV}}{2} \quad (32)$$

$$X_{cornerrr} = X_{pos} - \frac{Length_{LV}}{2}, Y_{cornerrr} = Y_{pos} - \frac{width_{LV}}{2} \quad (33)$$

where $X_{cornerrr}$ and $X_{cornerrl}$ are the X-positions of the rear right corner and rear left corner of the LV respectively while $Y_{cornerrr}$ and $Y_{cornerrl}$ are the Y-positions of the front right corner and the front left corner of the FV respectively.

Finally, it is assessed that the FV cannot avoid the collision with LV by steering to the left if within the prediction space,

$$X_{cornerfr} \geq X_{cornerrl} \;\&\; Y_{cornerfr} \leq Y_{cornerrl}, \text{ at time } t_i \quad (34)$$

Meanwhile, if the FV makes a decision to turn right, it cannot avoid the collision with the rear end of LV if within the prediction space,

$$X_{cornerfr} \geq X_{cornerrl} \;\&\; Y_{cornerfr} \geq Y_{cornerrr}, \text{ at time } t_i \quad (35)$$

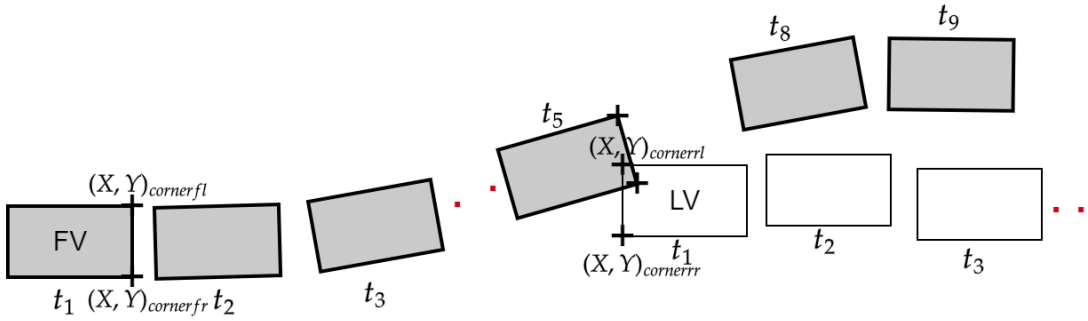

Figure 9 *The FV steers left but collides with the rear end of the LV. The above condition [34] collision is satisfied.*

5. *Extracting performance metrics:* If the FV collides with the LV at any time step t_i, then the loop of the assessment algorithm breaks. Thus, 'Latest point to Steer (LPS)' is identified and performance metrics of the FV at time step , t_{i-1} , such as TTS (time-to-steer) and TTC (time-to-collision), MD, Velocity, and Range between the two vehicles are computed and stored.

$$TTC = \frac{Range}{\Delta v} \tag{36}$$

where $\Delta v = velocity\ of\ LV - velocity\ of\ FV$

3 Results

This chapter presents the results obtained in the simulations from the collision avoidance assessment discussed in the previous section. Firstly, the performance metrics obtained from all three VDTs are plotted as data points. Next, a comparison of Time-to-Steer (TTS) and offset is made and a conclusion on their dependency is established for all three VDTs. Next, the comparison between the Maneuver Distance (MD) and Time-to-Collision (TTC) is made. Finally, the correlation between TTS and TTC is assessed. In Section 3.1, similar comparisons are made from sensitivity analysis only on one of the trajectories. Due to computational constraints only a limited amount of data points is considered in the results.

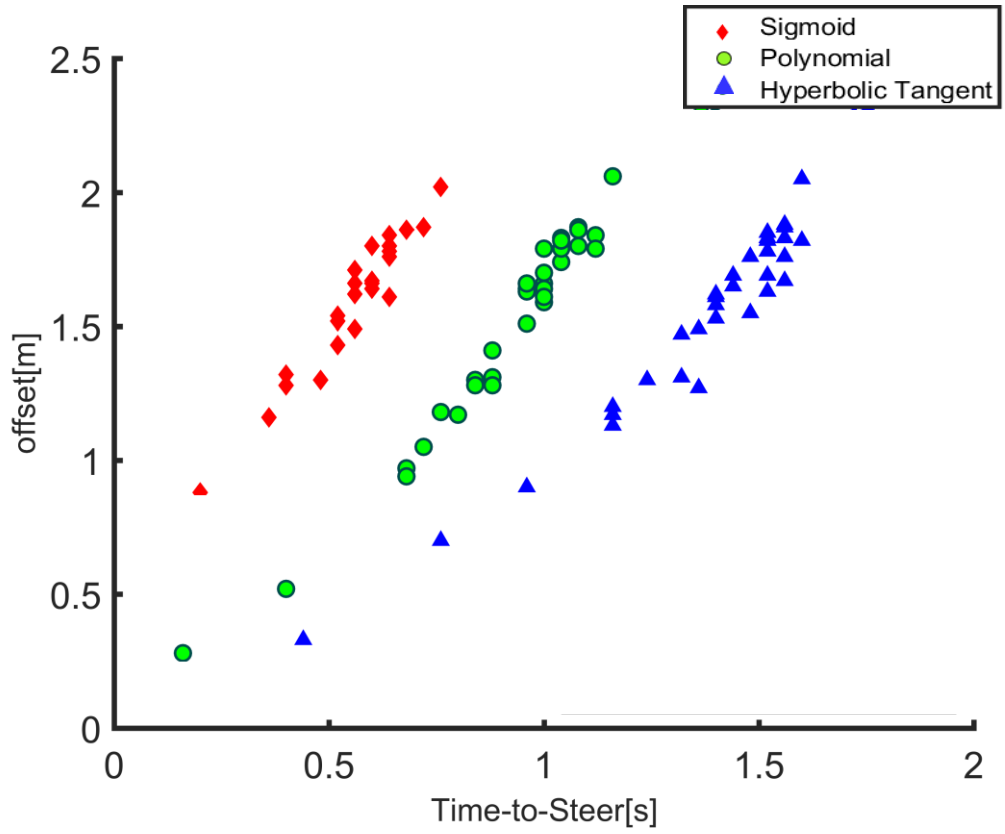

Figure 10 *Time-to-Steer vs Offset for sigmoid, polynomial and hyperbolic tangent trajectories respectively*

The plot above clearly indicates that the TTS is affected by offset in a linear trend, that is, the higher the offset, the higher is the TTS. Moreover, it can be seen that the sigmoid trajectory has the lowest TTS values compared to the fifth-order and hyperbolic tangent trajectories. Furthermore, for a given offset, it could be said that the sigmoid trajectory was quicker in response to reach that offset value compared to the other two VDTs.

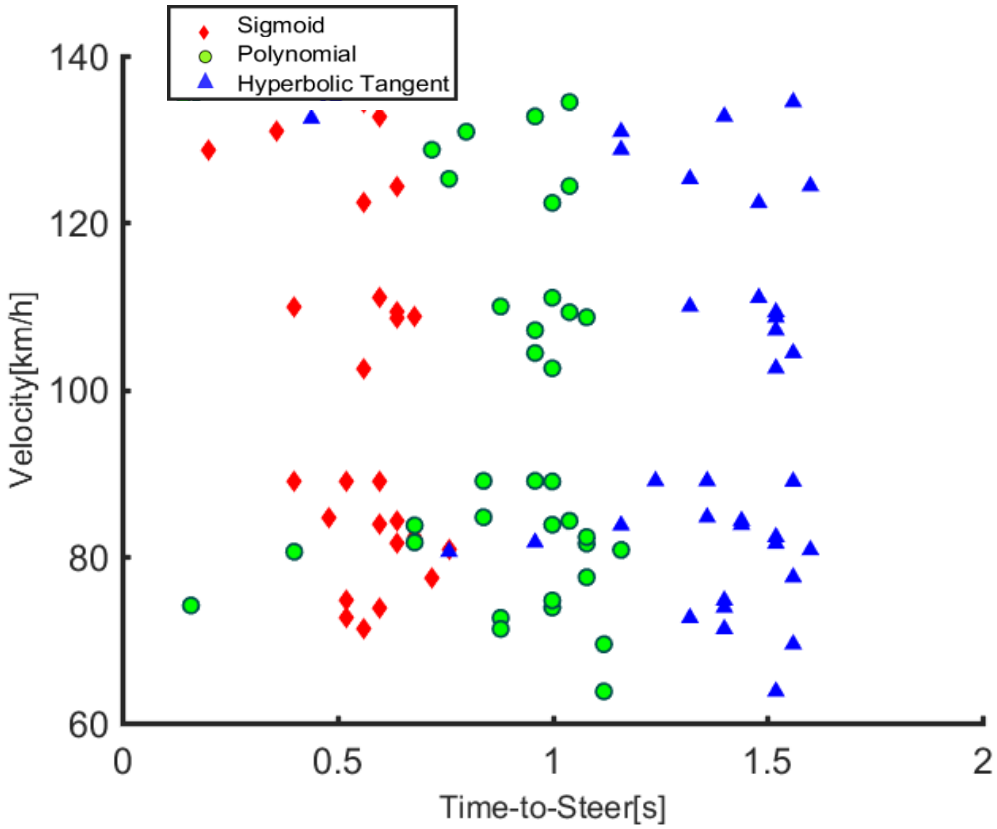

Figure 11 *Time-to-Steer vs Velocity for sigmoid, polynomial and hyperbolic tangent trajectories respectively*

From Figure 11, which represents TTS vs velocity, there is no obvious correlation between the two parameters. However, upon introduction of offset in the third dimension, the relation between the three can be clearly established.

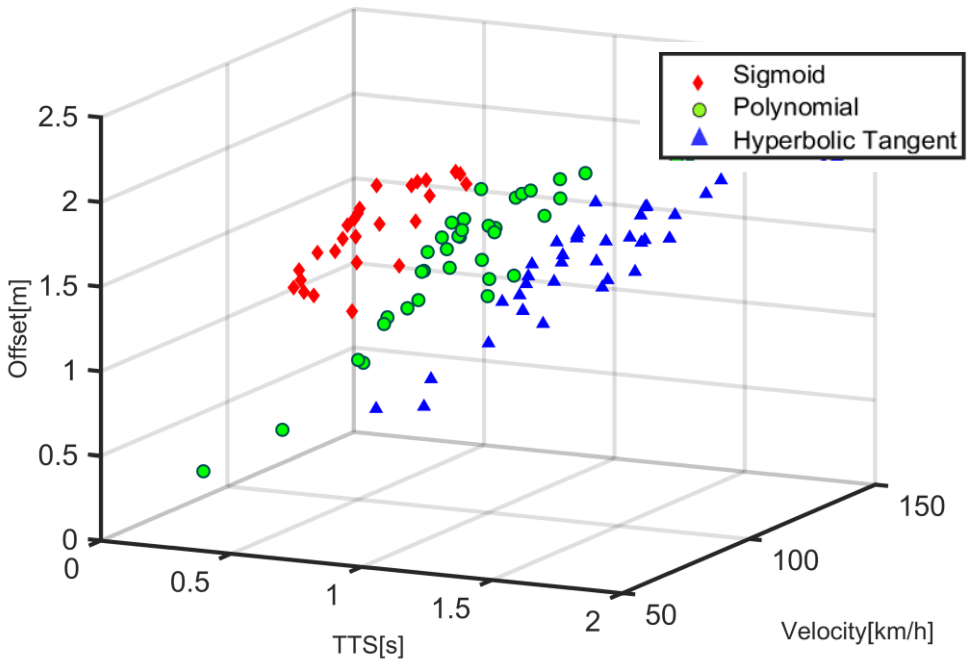

Figure 12 *Time-to-Steer vs Velocity vs offset for sigmoid, polynomial and hyperbolic tangent trajectories respectively*

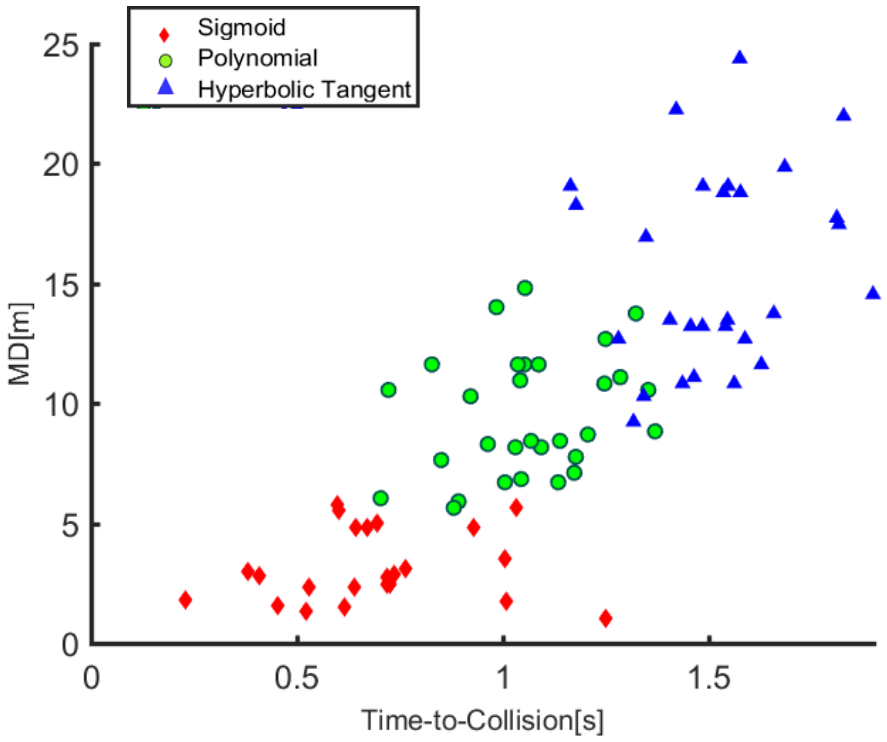

Figure 13 *Time-to-Collision vs Manuever Distance (MD) for sigmoid, polynomial and hyperbolic tangent trajectories respectively*

As manoeuvre distance (MD) decides the last point to steer, it can be established that as the shorter the MD is, the closer the FV gets with respect to LV. Which means that the TTC will be lower if the MD and relative speed are lower. It can be observed from the figure 13 that the distribution points for sigmoid is populated around the lower left corner of the plot, which corresponds to the lower MD values. The TTC values for the sigmoid lies between 0.2 to 1s, with MD values ranging from 2 to 5 meters. The distribution of TTCs for the polynomial trajectory lies in between the sigmoid and hyperbolic tangent trajectory corresponding to TTC 1 to 1.5s for MD ranging from 5 to 15 meters. The hyperbolic tangent trajectory has its points populated in the upper right region of the plot which corresponds to TTC values ranging from 1.5 to 2 s for MD varying between 15 to 20 meters.

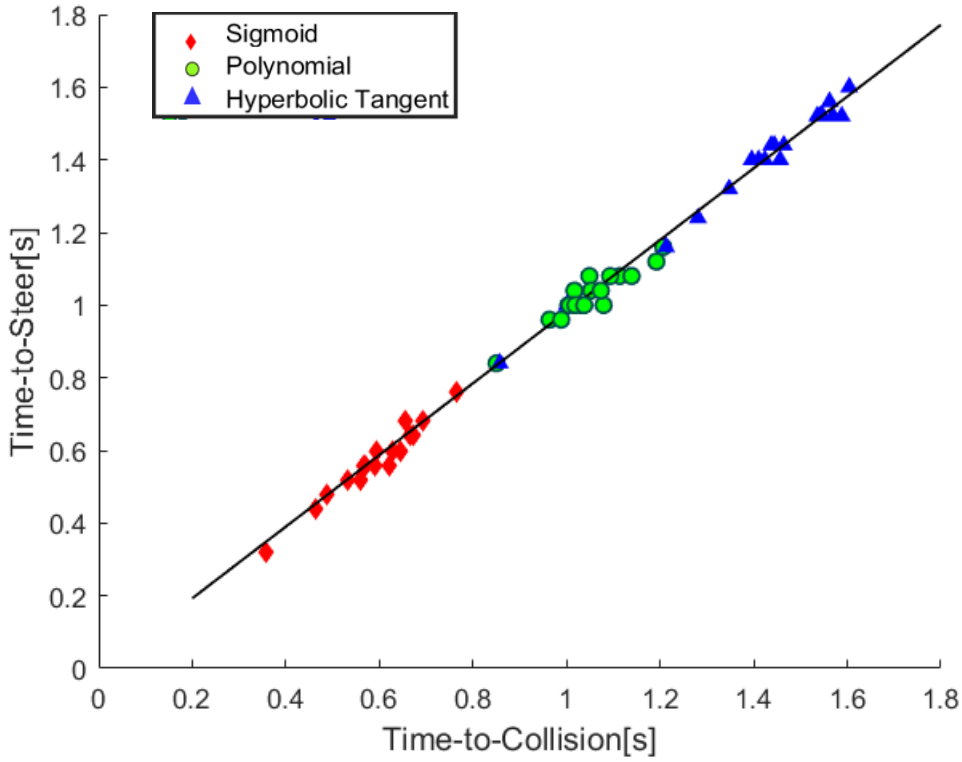

Figure 14 *Time-to-Collision vs Time-to-Steer for sigmoid, polynomial and hyperbolic tangent trajectories respectively*

Figure [14] shows that, as expected, there is a clear correlation between the TTCs and TTS for all three VDTs. Overall, it could, again, clearly be seen that as the shortest MD values correspond to the sigmoid trajectory, both TTC and TTS falls in the lower-left region of the plot ranging between 0.4 to 0.8s. A similar explanation could be established for the fifth-order polynomial trajectory where the TTS and TTC fall between 0.8s-1.2s and for hyperbolic tangent, the datapoints range between 1.2s-1.7s.

3.1 Sensitivity Analysis

In this section a sensitivity analysis is made on the single-track model used in this thesis work. The results from sensitivity analysis were extracted for three conditions:

- The lateral and longitudinal load transfer effect in the single-track vehicle model that were used for initial results was removed.
- The overall cornering stiffness of the axles were increased.
- The overall cornering stiffness of the axles were decreased.

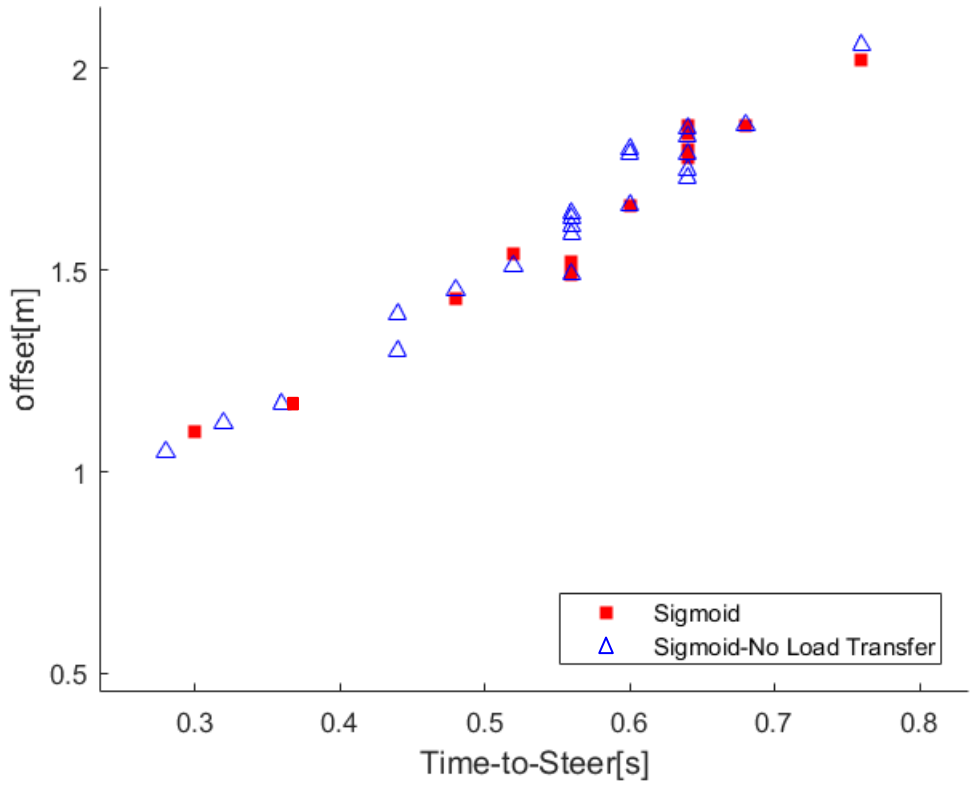

Figure 15 *Results of Time-to-Steer vs Offset when the load transfer is removed from the vehicle model for sigmoid trajectory.*

Figure [15] shows the simulation results on the sigmoid trajectory with and without both the lateral and longitudinal load transfer corrections. The figure shows that there was not much effect on the TTS values when the load transfer was removed from the vehicle model. The figure [16] below shows the lateral acceleration response of the vehicle with and without load transfer. Also, how the load transfer correction affects only the normal loads acting on the inner and outer wheels during a maneuver is revealed in the figure [17]. It is obvious that due to load transfer the normal loads acting on the outer wheels (6400 N and 4300 N respectively) are higher compared to the inner wheels (6750 N and 4400 N respectively). Also, it could be seen that the Figure 16 shows the lateral forces acting on the front and rear tires with and without the load

transfer effect. It could be clearly seen that in both cases the lateral force was approximately 2100 N.

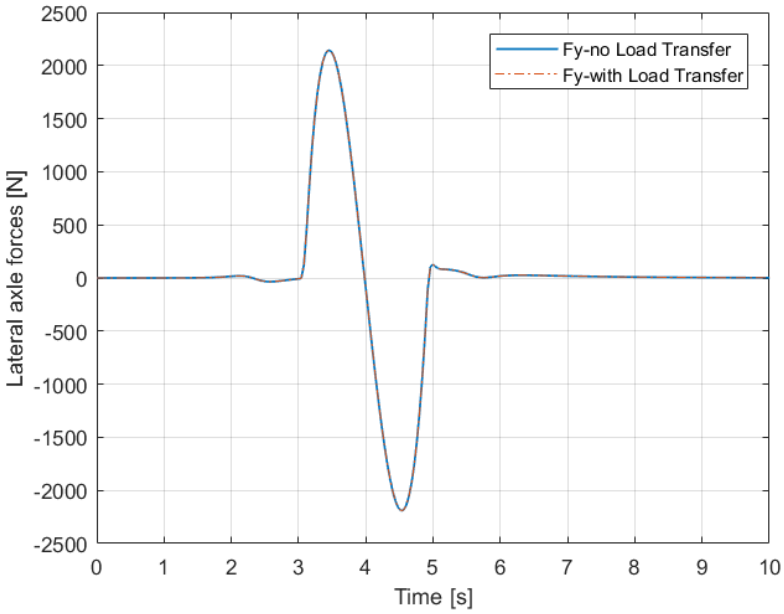

Figure 16 *Lateral forces acting on the front tire when the load transfer effect was removed (blue) and the lateral forces on front tire when the load transfer effect was considered (red).*

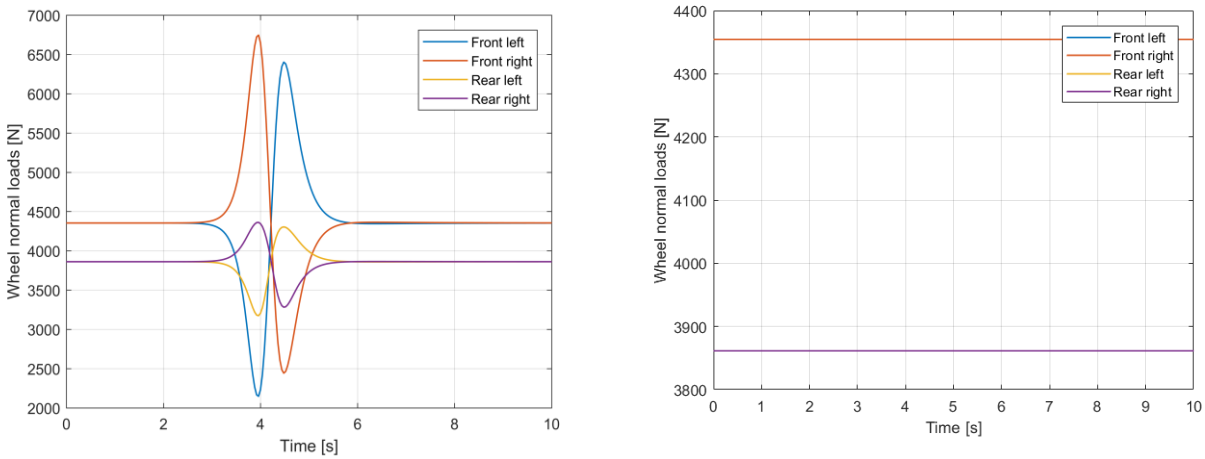

Figure 17 *Normal loads acting on the front and rear tires when the load transfer is included (left) and the image on the right shows the normal loads on the front and rear tires without load transfer.*

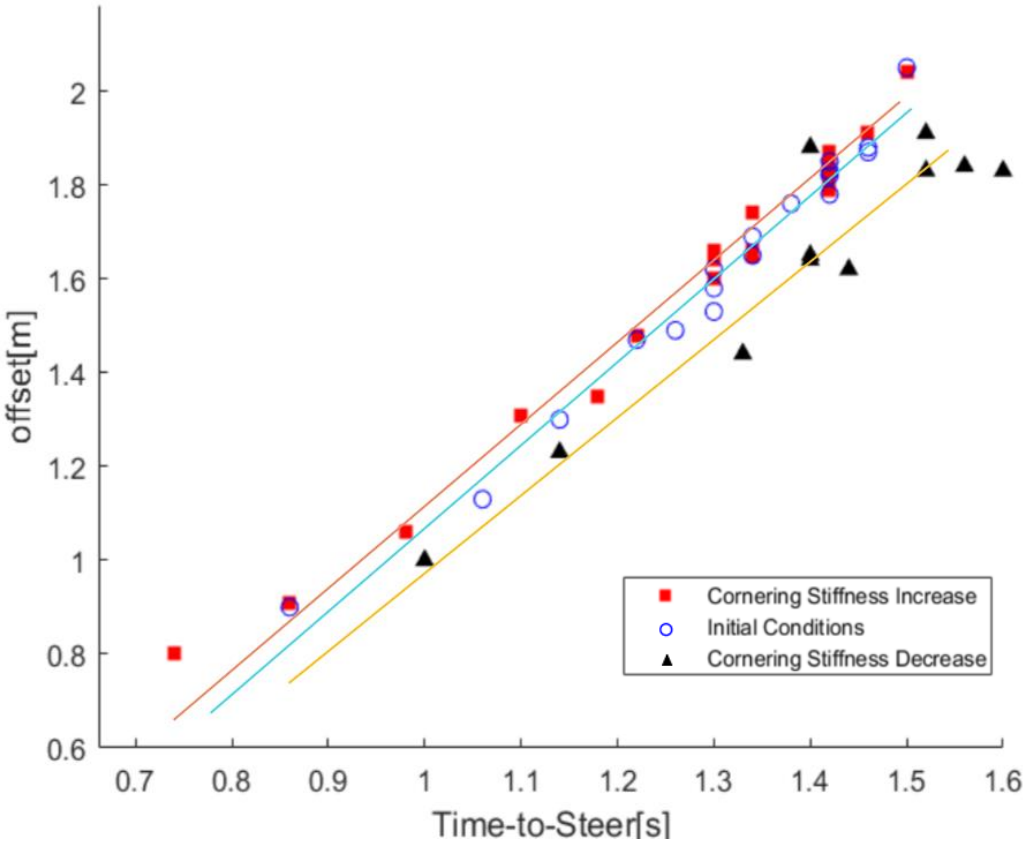

Figure 18 *Results of analysis when cornering stiffness of tires are changed and simulated on the hyperbolic tangent trajectory. A linear regression model is fitted all three simulation results. The slope is lower when cornering stiffness was decreased (1.1803) compared to the initial conditions (1.2450)*

Figure 18 represents the simulation results in terms of TTS and offset when the initial cornering stiffness was increased or decreased. The initial parameters of the vehicle model used were of the Saab 9-3 vehicle where the vehicle model was in "Neutral Steer" condition. To study the effects of understeer and oversteer of the vehicle, the cornering stiffness of the axles (rotating element connecting two tires) was first increased and then decreased respectively. For each a new set of simulations was performed. The red square dots in the Figure 18 represents the simulation results when the cornering stiffness of the axles was set to a higher value, to represent tire characteristics of a race car. The black triangles in the Figure 18 show how the TTS values were affected when the cornering stiffness of the axles was decreased. It is clear that TTS values increased compared to the results obtained with the initial conditions (represented by the blue circles) when cornering stiffness was decreased. Clearly, there is approximately 0.1s delay introduced when the cornering stiffness was decreased. Whereas when the cornering stiffness was increased, there were no obvious changes in TTS compared to the initial conditions.

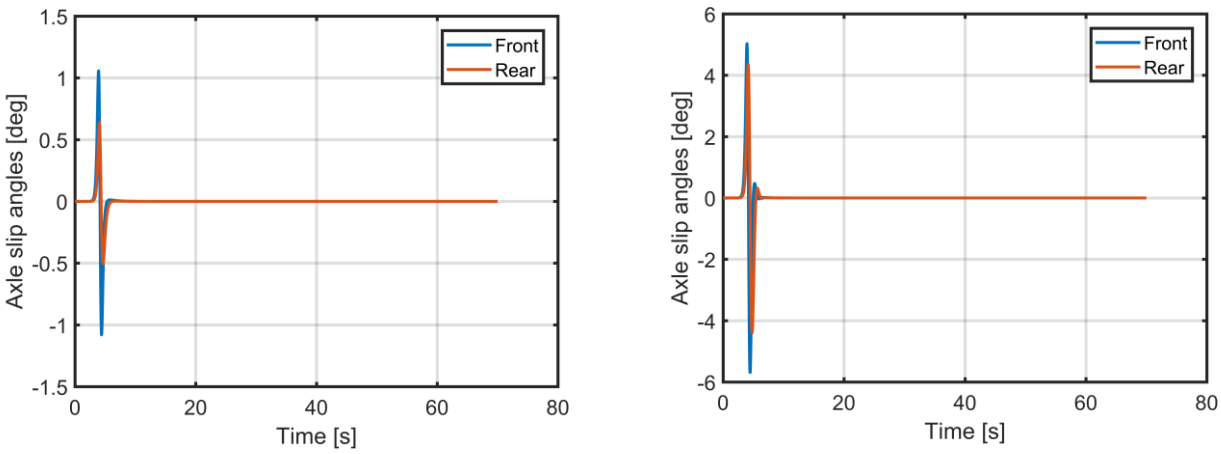

Figure 19 *Axle slip angles when cornering stiffness of tires are increased (left) and decreased (right) simulated on the hyperbolic tangent trajectory*

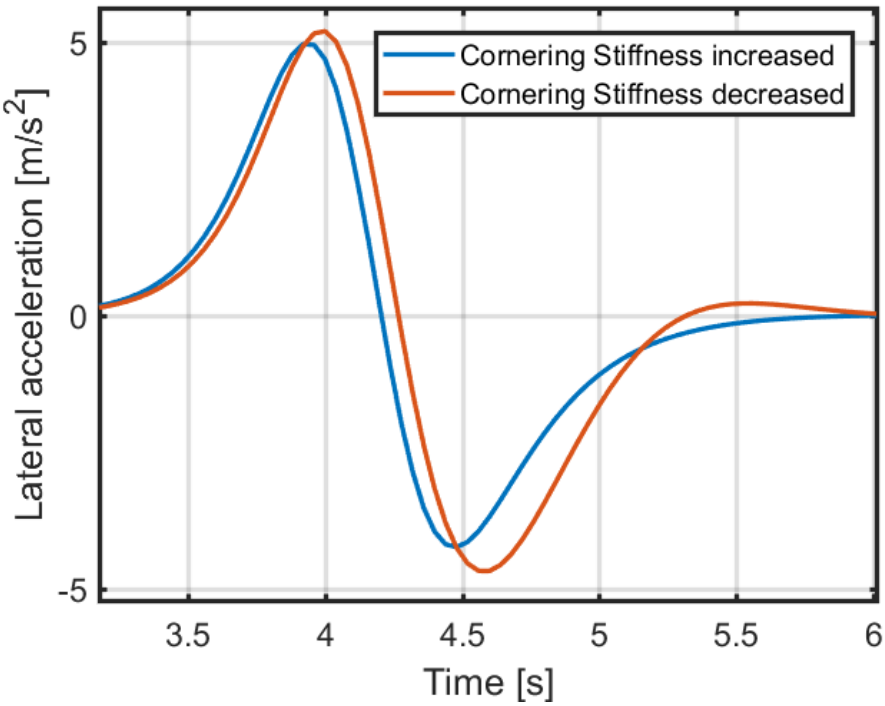

Figure 20 *Lateral acceleration response from the vehicle model when the cornering stiffness was increased and decreased. There is approximately 0.1s phase delay between the two responses.*

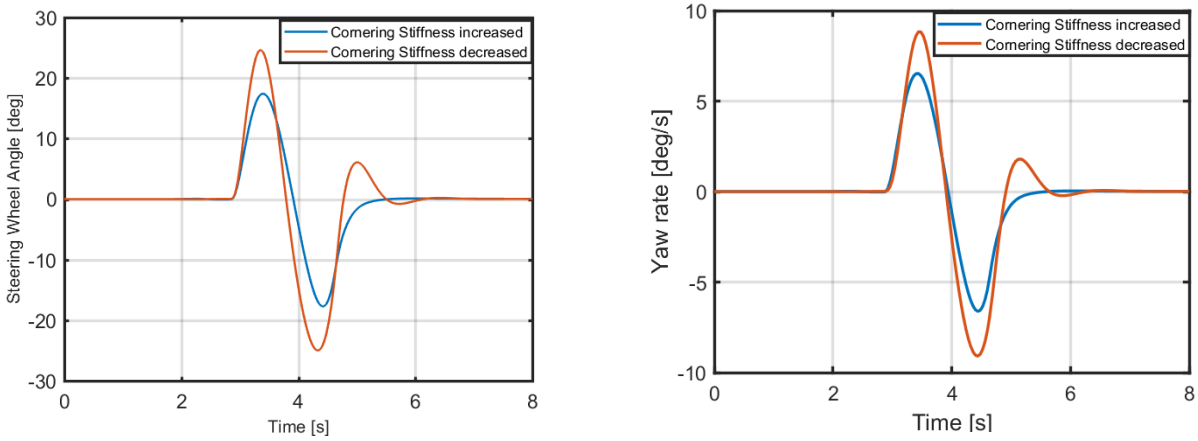

Figure 21 Steering wheel angle and Yaw rate response from the vehicle model when the cornering stiffness was increased and decreased

Figure 20 and Figure 21 reveals that there is a phase delay between the results when cornering stiffness was increased and decreased respectively. When the vehicle was maneuvering in oversteer condition, the required steering wheel angle was higher (25 degrees approximately) compared the condition when the vehicle was in understeer condition (17 degrees approximately). Also, the yaw rate response was comparatively higher in oversteer condition.

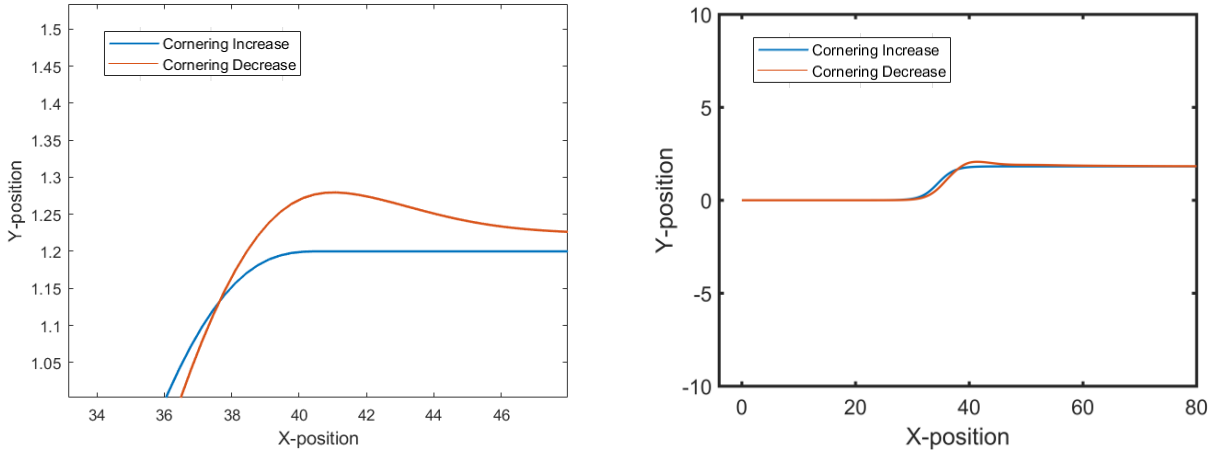

Figure 22 Results of the performance of the PID controller in understeer and oversteer condition

Figure 22 reveals that the PID controller introduced a slight overshoot in the vehicle trajectory when the vehicle was in oversteer condition. Compared to the condition in understeer (blue line), there was approximately 0.1 m of deviation from the offset (1.2 m).

4 Discussion

As mentioned earlier, the aim of this thesis is to study the impact of trajectory and steering model choice on crash avoidance timing by taking into account the drivers' comfort lateral acceleration in a simulation of rear-end conflicts. Three continuous curvatures (VDTs) were assessed with respect to avoidance timing as part of driver collision avoidance assessment that included drivers' comfortable steering as a constraint. A total of 86 rear-end crashes were used from the dataset for the assessment. For simulations, a single-track lateral dynamics model with load transfer effect was implemented in Simulink. Virtual simulations were made using the different VDTs and using a PID controller applied as a feed-back control, aiming to have the vehicle follow the VDTs, and to assess, in each time step, if the collision could be avoided within driver comfort lateral acceleration.

4.1 Data

After the initial evaluation of available data sources the decision was made to use information on generated crashes from highD [Olleja, 2019]. Other counterfactual simulation studies, such as have used other NDDs. For example, [Bärgman, 2015 used SHRP2 to create rear-end crashes based on driver behavior models. SHRP2 data was not accessible for this thesis work. Furthermore, not many NDDs are open to the public, unlike highD [Krajewski et al., 2018]. The information on the vehicle kinematics of the FV and the LV was accessible from the 86 created crashes by [Olleja, 2019] for the purpose of this thesis work. Moreover, the dataset was very suitable for extracting the parameters for evaluating three trajectories without having to introduce major assumptions. For example, to perform any kind of lane change, it is necessary to access the information like velocity and the lateral offsets. The simulation model was designed around these extracted parameters that provided the results as desired. Beyond that, this thesis also further validated the data quality of the generated crashes as major flaws in the information (for example, the X and Y positions of the vehicles) would have been revealed by affecting the simulation results.

4.2 Virtual Desired Trajectories (VDT)

This thesis is a contribution to driver collision avoidance assessment using steering that uses predefined trajectories. This is something used by several authors that have investigated steering vehicle dynamics, but with different objectives. [Schorn and Isermann, 2006] used a sigmoid equation [5] to develop a collision avoiding vehicle driver assistance system with steering, braking and a combination of steering and braking. The goal of their work was to evaluate emergency steering, where two feed-back controller approaches were used, to guide a vehicle on a desired sigmoid trajectory. Also, they used a non-linear two-track model for simulations and compared the results from the controllers with real test drives in terms of path-following control. [Pongsathom et al., 2019] used a hyperbolic tangent equation to perform a Double-Lange Change (DLC) test on lightweight vehicles. Their goal was to test a Direct Yaw Control system to compensate for the changes in vehicle dynamics (for example, loading conditions) using simulations and experimental studies. [Xiangkun He et al.,2018] used a fifth-order polynomial equation to design an emergency steering for

autonomous vehicles. A backstepping sliding mode controller was used to track the trajectory motivated by the polynomial equation. Three layers of the control architectures were motivated by [Xiangkun He et al.,2018] wherein a motion control layer, a lateral controller considers the non-linearity of the tires in emergency situations. It is assumed in this thesis that the PID controller is the driver feedback performing the avoidance maneuver considering comfortable limits and physical stability of the vehicle without any visual feed-back. Traditionally, the driver models have incorporated usage of the desired path using certain elements of control theory [Markula 2015]. In previous studies, the authors that have used these closed-loop systems with feedback control have compared the implementation of these controllers with human driving on test tracks. The results of those works show that the computer simulation results match with that of manual driving. The fundamental assumption was the driver performs an evasive maneuver with continuous error correction and this became essential in the decision to use a feedback controller. All vehicle control in the end may be considered closed-loop since the driver needs to react to the environment – but it is a much a matter of time-scale on the response. Actually, many driver behavior models have also been previously motivated considering near-crash behavior of driver [Sharp et al. 2000, MacAdam 1981, Gordon and Magnuski 2006, Salvucci and Gray 2004, Markula 2015]. Such models implemented parts of this closed-loop driving as discrete open-loop steering behavior in near-crash conditions. [Markula 2015] in his thesis has compared many driver models (open-loop and closed-loop) and has suggested that there are several competing driver models for a given scenario but also, that which reproduces the best human driver behavior still needs further investigation.

The performance metrics used in this thesis can be compared with an experiment by [Markula 2015]. In the experiment, a 24-subject driving simulator study was designed where the truck drivers were exposed to rear-end conflicts with an unexpected rear-end scenario, wherein, a higher speed lead-vehicle overtaking and braking for no reason. It was observed that most drivers performed the avoidance steering when the TTCs were between 2 and 3 seconds. The TTC and TTS distributions in this thesis work range from 0.6s to 1.5s, clearly much lower than the driver behavior captured in the [Markkula 2015] study. However, the [Markkula 2015] study did not cover the reason behind the kinematic urgency or the stimuli to which the drivers reacted to the conflicts and was experimented on a simulator rather than a real-world scenario.

The characteristics of the curvatures of the three VDTs are a major contributor to the difference recorded between the results of each of these in terms of collision avoidance timing which is approximately 0.5s. On comparison, the sigmoid VDT has weaker gradients (derivatives) than the hyperbolic tangent VDT whose derivatives are much stronger. In addition to this, it is observed that the fifth-order polynomial falls between the characteristics of those of sigmoid and hyperbolic. Furthermore, this observation is also evident from the simulation results in terms of MD values, explaining the differences in a thorough manner. The sigmoid tangent resulted in the lowest range of values of MD, that is, 2 to 5m, whereas, the hyperbolic tangent resulted in much higher MD values like 15 to 20m. The TTC distributions with respect to MD (see figure 13) for each VDT reveals the point (defined as “Last point to Steer”) at which the driver performed the evasive manoeuvre within the comfort limits. Interestingly, a relation could be established between these results and in a more recent study on naturalistic driver reactions on rear-end conflicts.

[Markula et al. ,2016] uses naturalistic driver behavior in near-crashes and rear-end crashes from SHRP2. In their work, [Markula et al. ,2016] uses a concept of visual looming to define the measurement of kinematic urgency by measuring a quantity called τ^{-1} (the ratio between optical expansion rate and optical size). The measurements were made based on off-road glances relative to leading vehicle and reaction time was recorded when the looming reached a certain threshold. On average, [Markula et al. ,2016] found that most driver reaction times for 'eyes-off-threat' were short, generally, below 1s. The crashes in the highD data were created under the assumption that the driver was not looking at the road when the LV started braking and as asserted previously, this thesis assumes that the avoidance manoeuvre is performed without any visual feed-back. With this assumption, it could be said the TTS distributions for sigmoid VDT fits the range of reaction times from [Markula et al. ,2016] study. Although the current work does not include such driver reaction times in the simulations, overall, it could be said that the selection of vehicle trajectory plays an important role to assess the safety of systems that include evasive steering virtually.

4.3 Sensitivity Analysis

The simulation results from the sensitivity analysis were reported/considered only in terms of TTS. As the performance metrics are all interdependent, considering each single one was not of particular importance here. In the first set of results where the load-transfer effect was removed, it is evident that the TTS values were only little or not impacted at all, compared to the cases when load-transfer was included in the vehicle model. The load transfer between the left and the right tires had an impact on the normal loads (see figure 17) but did not affect the lateral forces (see figure 16) acting on them, and consequently not the TTS. This further means that the load-transfer when included in a single-track lateral dynamics model, does not introduce any major changes in collision avoidance timing except for a few milliseconds of difference that were seen compared to a single-track model without load-transfer. This is at least true when only studying comfortable steering avoidance, as was performed in this thesis. For avoidance manoeuvres reaching the physical limits of the vehicle (lateral acceleration close to 1g), it may be different as the inner wheels experience a lift

Finally, when the axle cornering stiffness was increased, the vehicle showed the understeer effects. This can be explained by the well-known relationship between the required steering angle and understeer gradient given by,

$$\delta = n \cdot (L + \mathrm{K} \cdot v^2) \cdot \kappa \tag{37}$$

where 'K' is known as the understeer gradient given by,

$$K = \frac{w_f}{C_f} - \frac{w_r}{C_r} \tag{38}$$

where w_f is the weight distribution on the front and w_r is the weight distribution on the rear of the FV. The value of K decides the in-built design of the vehicle in terms of additional steering angle per increase of lateral force or lateral acceleration during

steady-state cornering [Bengt Jacobson et al, 2019]. If K>1 the vehicle is said to be understeered, neutral steered if K=0 and oversteered when K<0. Practically, most vehicle manufacturers design vehicles to be understeered as oversteer causes instability. The hypothesis first established in section 1.1 was based on this relationship. When the axle cornering stiffness was increased, the value of K was observed to be positive. Consequently, this caused the vehicle to be in an understeer condition. As per observations suggest from Figure [18], the majority of TTS values were nearly the same as simulation results when the vehicle was initially in a neutral steer condition. However, when simulations with a decrease in the cornering stiffness was performed, the simulation results showed some difference from the original cornering stiffness, in terms of TTS values. That is, there was an increase in TTS values compared to the initial conditions. As the understeer gradient was observed to be negative, the vehicle was set to be operating in an oversteer condition.

A better explanation may be offered by using the other parameters of the vehicle's response in simulations when it is in understeer and oversteer condition as the K value only gives a hint of the vehicle's in-built design. Firstly, a vehicle is said to be in an understeer condition if the front slip angle is greater than the rear slip angle. The figure [19] also corresponds that the front slip is more. The relationship between the slip angles, K and the lateral acceleration is given by,

$$\alpha_f - \alpha_r = K \cdot \frac{ay}{g} \tag{38}$$

Considering that the difference in the side slip angles is always positive, the rear slip angle should be more than the front slip angle given that the value of K<0, that is, if the vehicle is in oversteer condition, the rear slip angle is more than the front. This is evident from the plot in the figure [19] where the rear slip angle is nearly equal to the front slip angle. The vehicle in the oversteer condition also introduced a higher lateral acceleration compared to the vehicle in understeer condition. Also, from the figure [21], the steering wheel and yaw rate response of the vehicle when cornering stiffness was increased for a given velocity is comparatively lower than the condition when cornering stiffness was decreased.

The results from the simulations, when the cornering stiffness was decreased, approximately increased the overall TTS values by only 0.1s. There was a phase delay in terms of vehicle response (yaw rate, lateral acceleration, etc.) compared to the original simulation results. Hence, there was no notable effect on the overall performance metrics during the collision avoidance assessment. This is due to the fact that the operating gains for the PID for a given velocity and offset were robust enough to produce the desired results with minimal lateral deviation between the VDT and the PID controlled path. That is, it reflects that a good driver performed the evasive maneuver avoiding the rear-end conflict. Also, the simulations were made under the assumption that the road condition was dry asphalt with a friction coefficient of 0.8. Given the weather or road conditions in the dataset and also the loading conditions, the performance metrics are considerably different. Also, generally the driver feed-back is not controlled when the vehicle maneuvers in oversteer condition. This suggests that the operating gains of the feed-back controller is of key importance for virtual simulations and should be set up in such a way that they provide robust performance under any given condition to compensate for larger delays in terms of TTS.

Furthermore, when the load transfer effect was removed for the simulations in sensitivity analysis, the TTS values remained nearly the same as the original results. This is due to the fact that the wheels cornering stiffness vary degressively with normal loads [Bengt Jacobsson et al., 2017] . During load transfer, the loss in the inner wheels in terms of cornering stiffness was not significant enough to affect the gain on the outer wheels due to which the TTS values were not affected when the load transfer was removed. Another reason is also that the model assumes the rigid suspension design which resulted in steady roll and pitch effects. In summary, it could be said that for such virtual assessment for driver collision avoidance within comfort limits, the load transfer effect did not play a major role although this is only due to certain assumptions made in this thesis, for example, the roll stiffness distribution. If the constraint of the driver comfort limit was ignored the results could possibly be more obvious.

4.4 Model and Parameter Choice for Virtual Assessment

The previously described observations in simulation results raise the question of what vehicle model and parameter settings would be the best choice to perform a virtual assessment for collision avoidance using steering. For answering this question, this thesis' simulations are categorized into four configurations in a first step.

Configuration	*A*	*B*	*C*
Analysis Type	Cornering stiffness increased	Cornering stiffness decreased	No lateral and longitudinal load transfer
Results	The TTS values remained unaffected	The TTS values increased by few milliseconds to a maximum of 0.1s	The TTS values remained unaffected

The vehicle model in *Configuration A* resulted in an understeer condition in the vehicle model which scarcely affected the TTS values. Whereas in *Configuration B*, the decrease in cornering stiffness caused the vehicle to oversteer and in turn increased the TTS values. The exclusion of the load transfer effect from the single-track model did not change the TTS values when the model was simulated in its initial conditions. Among the three configurations used in this thesis work, *Configuration A* is best suitable for virtual assessment integrated into a single-track model as the *Configuration B* would produce undesirable oversteer behaviour of the vehicle and does not cope with real-world comfortable driving. Moreover, oversteer vehicles would motivate the need to include an ESC (Electronic Stability Control) for better stability and this would increase the complexity of the virtual assessment. As previously discussed, the load transfer effect had no or light effects on the overall results. Hence this choice of configuration is not recommended for such an assessment in a single-track model considering driver comfort lateral acceleration as it did not considerably reflect the vehicle cornering responses. Future work needs to extend this to a complex two-track

lateral dynamics model to capture such load-transfer effect intensely - to see if there is an influence on the performance metrics with such more advanced models. Furthermore, the choice of a PID controller, over other types of controllers used in previous studies, was suitable to perform the simulations on the collision avoidance assessment although the PID created minor lateral deviations in results from *Configuration B*. However, the use of closed-loop models for steering behavior needs more evidence on how well it represents real driving behavior in near-crash conditions. As mentioned previously, near-crash behavior is often modeled as open-loop maneuvers [Markkula, 2015].

Finally, it has to be considered that when evaluating a simulation's results, those are crucially affected by the underlying data choice as well. In this case, the highD crash dataset contained the major parameters for the model, yet more information like individual driver information, weather conditions, and the vehicle loading conditions would have added more quality to the results

5 Limitations and Future Work

One of the major limitations of this thesis work is the computation time of the collision avoidance assessment. The main reason for the longer computation time is due to the implementation of the lateral dynamics model in Simulink. This would require additional computational power to run Simulink efficiently and select an optimal solver that performs faster computations. The inclusion of the Newton-Bisection method is another limitation that added to the higher computation time. It is one of the simplest and effective root-finding methods. However, the dataset in the highD rear-end crashes had many samples to be assessed in real-time and at each time step sometimes more iterations required to satisfy the convergence criteria through the Newton-Bisection process. The next limitation is the tuning process of the PID controller through the automatic tuning option. The automatic tuning function available in the Simulink did not provide sufficient results and manual tuning was used extensively instead of other alternative control strategies like Zeigler-Nichols method [Kushwah et al., 2014] or Cohen-Coon method [Olaiya O. O et al., 2018]. However, the tuning gains obtained from the manual method were not robust enough to perform the simulations when the cornering stiffness was decreased.

Another drawback of the PID is the lower operating speed ranges. It was noticed that the PID introduced aggressive characteristics to the output at lower speeds of the FV ranging from 20 to 40 km/h. At these operating speeds, the PID could not track the VDT as the response time from the PID was too slow and hence a higher steering wheel torque would be necessary to be applied. Therefore, the crash cases with speeds ranging from 20 to 40 km/h were ignored. Furthermore, the proposed collision detection method in the collision avoidance assessment was found to be effective although the accuracy of this method could have been better if the FV and the LV were modeled as two rectangles to check if there was an overlap of the rectangles a collision would have been detected.

The highD data posed a couple of shortcomings in that only kinematics from created crashes were made use of and there was no access to any real-world kinematics in the dataset. Furthermore, it did not comprise of information on road or weather conditions, or any physical loading conditions. Inclusion of this data would have had a major impact on the overall results in the virtual assessment.

Based on the above limitations highlighted, the following future work is proposed:

- Firstly, this thesis work only focuses on avoidance assessment using steering maneuver in rear-end conflicts with lateral acceleration as driver comfort limit. An interesting study would be to include collision avoidance assessment for braking with longitudinal acceleration as driver comfort limit.
- The implementation of this thesis work did not include an AES algorithm to perform automatic interventions using steering. [Hillenbrand et al., 2006, Brännström et al., 2008, Carlo Ackermann et al.,2014] proposed AES and AEB algorithms for automatic interventions using steering and braking where each work used different performance metrics for evaluation. These implementations could be used as inspirations for further research of the current thesis work.
- A potential improvement that could be implemented is replacing the Newton-Bisection method with more efficient approach to find the MD. Genetic Algorithm is a well-known optimization method by, for example, J.H. Holland, which could be used in the current thesis work to find the optimal MD for a given velocity and offset. Time constraints prohibited the use of genetic algorithms.
- As highlighted previously, the use of PID controller in this thesis had its drawbacks in certain operating conditions. An improvement would be to test the implementation with other types of controllers. For example, [Masayoshi Tomizuka,1994] proposed many types of lane change trajectories in his work and used different types controllers such as sliding-mode, LQ and FSLQ controller as a feed-back. A similar approach could be made to compare PID with other controllers to propose a robust feed-back controller. Also,
- The use of feed-back controller acting on the steering wheel in the current work was assumed to be the operating as a driver who steers to avoid a rear-end conflict. It would be an interesting approach to evaluate open-loop steering without inclusion of a feed-back controller. This open-loop steering could replicate the steering wheel action that results in a trajectory similar to the near-crash behaviour in real-world driving.
- Finally, with the same focus as current research, to extract the results more realistically to a real-world vehicle, a two-track vehicle model with a suspension linkage could be used. The load-transfer effect in a two-track model is more notable as a consequence of body roll effects.

6 Conclusion

In this thesis work, three continuous curvatures, called VDT, were used to perform virtual collision avoidance assessment on rear-end crashes (created) from the highD dataset. These curvatures were previously used in studies that integrated them in closed-loop control. This thesis used a similar approach controlling these desired VDTs using a PID controller. The aim of this thesis is to study the impact of these VDTs, and other choices in the lateral vehicle model, on collision avoidance timing. A single-track vehicle model with load transfer effect was used to perform the simulations. A sensitivity analysis was performed by modifying certain parameters in the vehicle model like cornering stiffness and removal of load-transfer effect. The overall focus of the work was about understanding the impact of the choice of driver avoidance maneuver, vehicle steering model and parameter settings required to perform virtual safety assessment of driver collision avoidance using steering. It was found from the simulation results that the sigmoid VDT resulted in lower collision avoidance timing ranging from 0.2-0.6s while fifth-order polynomial VDT resulted in 0.5-1.2s and hyperbolic tangent VDT resulted in 1.2-1.5s, respectively. The sensitivity analysis results showed that when the cornering stiffness of the tires was decreased, a minor delay of 0.1s. was introduced in the collision avoidance time but the increase in cornering stiffness did not introduce any changes compared to the original simulation results. Upon removal of lateral and longitudinal load-transfer effect, the transient response (yaw rate, lateral forces, lateral acceleration, etc.) of the vehicle did not change compared to the model with load-transfer. Overall, differences between the simulation results between the VDTs were found to be relatively large (0.5s) in relation to the driver reaction times in near-crash behaviors made in previous research works. When the cornering stiffness was decreased, the PID controller introduced a slight lateral deviation that accounts to 0.1s increase in TTS values compared to the original simulations. These results were also due to the assumption that the road condition was dry with friction coefficient of 0.8 (full traction) to which the PID provided robust performance. The overall results in the virtual simulations would be more realistic (correct?) if the information of road conditions were available in the highD dataset. The single-track vehicle model could not capture the effect of rolling as only a rigid suspension was used and the width of the vehicle is neglected in the mathematical model. Due to which the simulation results did not show any deviation and require an enhanced two-track model in future work to examine the results.

7 References

Ahmed, K. I., 1999. Modeling Drivers' Acceleration and Lane Changing Behavior. PhD thesis. Massachusetts Institute of Technology, Cambridge, Mass.

Alvarez, S., Page, Y., Sander, U., Fahrenkrog, F., Helmer, T., Jung, O., Hermitte, T., Düering, M., Döering, S., Op den Camp, O., 2017. Prospective Effectiveness Assessment of ADAS and Active Safety Systems Via Virtual Simulation: A Review of the Current Practices, in: 25th International Technical Conference on the Enhanced Safety of Vehicles (ESV). Detroit, MI, pp. 1–14. https://www-esv.nhtsa.dot.gov/Proceedings/25/25ESV-000346.pdf

Bärgman, Jonas, 2015. On the analysis of naturalistic driving data.

Bärgman, Jonas, 2016. Methods for Analysis of Naturalistic Driving Data in Driver Behavior Research.

Bärgman, J., Boda, C.N., Dozza, M., 2017. Counterfactual simulations applied to SHRP2 crashes: The effect of driver behavior models on safety benefit estimations of intelligent safety systems. Accid. Anal. Prev. 102, 165–180. doi:10.1016/j.aap.2017.03.003

Bekiaris, E., Petica, S. & Brookhuis, K, 1997. "Driver Needs and Public Acceptance Regarding Telematic In-Vehicle Emergency Control Aids", In: Brookhuis, K. A., De Waard, D. (1999), "The Human Factor in Advanced Driver Assistance Systems", Seminar Publication on Advanced Driver Assistance Systems, Paper No S653/007/99, The Automatic Division of The Institution of Mechanical Engineers, Professional Engineering Publishing

Bellem, Hanna & Seitz, Barbara & Schrauf, Michael & Krems, Josef., 2018. Comfort in automated driving: An analysis of preferences for different automated driving styles and their dependence on personality traits. Transportation Research Part F Traffic Psychology and Behaviour. 55. 10.1016/j.trf.2018.02.036.

Bengt Jacobson et al, 2017. Vehicle Dynamics Compendium, Division of Vehicle and Autonomous Systems, Department of Applied Mechanics, Chalmers University of Technology, www.chalmers.se

Benjamin Coifman, Lizhe Li, 2017. A critical evaluation of the Next Generation Simulation (NGSIM) vehicle trajectory dataset,Transportation Research Part B: Methodological,Volume 105 ,Pages 362-377,ISSN 0191-2615, https://doi.org/10.1016/j.trb.2017.09.018. (http://www.sciencedirect.com/science/article/pii/S0191261517300838)

Benmimoun, Mohamed & Ljung Aust, Mikael & Faber, Freek & Zlocki, Adrian & Saint Pierre, Guillaume, 2011. Safety analysis method for assessing the impacts of advanced driver assistance systems within the european large scale field test Eurofot.

Bliss, James & Acton, Sarah, 2003. Alarm mistrust in automobiles: How collision alarm reliability affects driving. Applied ergonomics. 34. 499-509. 10.1016/j.apergo.2003.07.003.

Brännström, M., Coelingh, E., Sjöberg, J., 2014. Decision-making on when to brake and when to steer to avoid a collision. Int. J. Veh. Saf. J. Veh. Saf. 7 1 , 87–106. doi:10.1504/IJVS.2014.058243

Brännström, M., Coelingh, E., Sjöberg, J., 2010. Model-based threat assessment for avoiding arbitrary vehicle collisions. IEEE Trans. Intell. Transp. Syst. 11 3 , 658–669. doi:10.1109/TITS.2010.2048314

Brännström, M., Sjöberg, J., Coelingh, E., 2008. A situation and threat assessment algorithm for a rear-end collision avoidance system. IEEE Intell. Veh. Symp., 102–107. doi:10.1109/IVS.2008.4621250

Carsten, Oliver & Nilsson, Lena, 2001. Safety Assessment of Driver Assistance Systems. European Journal of Transport and Infrastructure Research. 1. 10.18757/ejtir.2001.1.3.3666.

Chee, Wonshik & Tomizuka, Masayoshi, 1994. Vehicle Lane Change Maneuver In Automated Highway Systems. Institute of Transportation Studies, UC Berkeley, Institute of Transportation Studies, Research Reports, Working Papers, Proceedings.

EuroFOT - European Field Operational Test, 2009. http://wiki.fot net.eu/index.php/EuroFOT

Ehiwario, J.C.. (2014). Comparative Study of Bisection, Newton-Raphson and Secant Methods of Root- Finding Problems. IOSR Journal of Engineering. 4. 01-07. 10.9790/3021-04410107.

Eidehall, A., Pohl, J., Gustafsson, F., Ekmark, J., 2007. Towards autonomous collision avoidance by steering. IEEE Transactions on Intelligent Transport System. 8 1, 84–94. doi:10.1109/TITS.2006.888606

FACS, Prof. (2012). Abbreviated Injury Scale. 10.1007/978-3-642-00418-6_355.

He, Xiangkun & Yulong, Liu & Lv, Chen & Ji, Xuewu & Liu, Yahui, 2018. Emergency steering control of autonomous vehicle for collision avoidance and stabilisation. Vehicle System Dynamics. 57. 1163-1187. 10.1080/00423114.2018.1537494.

Hillenbrand, J., Spieker, A.M., Kroschel, K., 2006. A Multilevel Collision Mitigation Approach - Its Situation Assessment, Decision Making and Performance Tradeoffs, IEEE Transactions on Intelligent Transportation Systems, Vol. 7, No. 4, pages 528-540, IEEE. doi:10.1109/TITS.2006.883115

Joseph, E. A, Olaiya O. O, 2018. Cohen-Coon PID Tuning Method: A Better Option to Ziegler Nichols-Pid Tuning Method. ISSN (Paper)2222-1727 ISSN (Online)2222-2863

Lee, J. D., and See, K. A. ,2004. "Trust in Technology:Designing for Appropriate Reliance," *Human Factors*, Vol. 46, No. 1, pp. 50–80.

Olson, P. L., & Sivak, M, 1986. Perception-response time to unexpected roadway hazards. Human Factors, 28, 91-96.

Karjanto, Juffrizal & Md Yusof, Nidzamuddin & Terken, Jacques & Delbressine, Frank & Hassan, Muhammad & Rauterberg, Matthias, 2017. Simulating autonomous driving styles: Accelerations for three road profiles. MATEC Web of Conferences. 90. 01005. 10.1051/matecconf/20179001005.

K.-E. Arz_en, 1999. A simple event-based pid controller," in Proc. 14th IFAC World Congress,vol. 18, pp. 423-428.

Knipling, R. R., 2015. Naturalistic driving events: No harm, no foul, no validity Proceedings of the 8th International Driving Symposium on Human Factors in Driver Assessment, Training and Vehicle Design Snowbird, Salt Lake City, UT. (pp. 197-203).

Krajewski, R., Bock, J., Kloeker, L., Eckstein, L., 2018. The highD Dataset: A Drone Dataset of Naturalistic Vehicle Trajectories on German Highways for Validation of Highly Automated Driving Systems. IEEE 21st International Conference on

Kushwah, Manoj, and Ashis Patra, 2014. "Tuning PID controller for speed control of dc motor using soft computing techniques-a review." Advance in Electronic and Electric Engineering 4.2: 141-148

Lewis-Evans, B., 2012. Testing models of driver behaviour PhD thesis, University of Groningen

Lindgren, A., 2007. Driving safe in the future? : driver needs and requirements for advanced driver assistance systems. Chalmers tekniska högskola.

Lindgren, A., 2009. Driving Safe in the Future - HMI for Integrated Advanced Driver Assistance System.

Ljung Aust, Mikael, 2012. Improving the Evaluation Process for Active Safety Functions.

Markkula, G., 2015. Driver behavior models for evaluating automotive active safety: From neural dynamics to vehicle dynamics.

Markkula, Gustav & Engström, Johan & Lodin, Johan & Bärgman, Jonas & Victor, Trent., 2016. A farewell to brake reaction times? Kinematics-dependent brake response in naturalistic rear-end emergencies. Accident Analysis & Prevention. 95. 209-226. 10.1016/j.aap.2016.07.007.

Neale, V.L., Dingus, T.A., Klauer, S.G., Sudweeks, J., 2005. An overview of the 100-Car naturalistic study and findings. National Highway Traffic Safety Administration United States.
https://www.nhtsa.gov/sites/nhtsa.dot.gov/files/100car_esv05summary.pdf

Nelles, O., 2001. Nonlinear System Identification. Springer-Verlag. Berlin.

NHTSA, 2003. Driver Attributes and Rear-end Crash Involvement propensity, National Center for Statistics and Analysis Advanced Research and Analysis

Parasuraman, R., & Riley, V., 1997. Humans and Automation: Use, Misuse, Disuse, Abuse. Human Factors, 39(2), 230–253. https://doi.org/10.1518/001872097778543886

Pacejka,H, 2012. Tire and vehicle dynamics. Retrieved from https://ebookcentral.proquest.com

Pierluigi Ollja, 2019. Assessment of AEB algorithms and relevance of datasets used for AEB assessment- https://odr.chalmers.se/handle/20.500.12380/300480.

Raksincharoensak, Pongsathorn & Daisuke, Sato & Lidberg, Mathias., 2019. Direct Yaw Moment Control for Enhancing Handling Quality of Lightweight Electric Vehicles with Large Load-To-Curb Weight Ratio. Applied Sciences. 9. 1151. 10.3390/app9061151.

Ranjitkar, Prakash & Nakatsuji, Takashi & Azuta, Yoichi & Senadeera, Gemunu & Lecturer, Gurusinghe. (2003). Stability Analysis Based on Instantaneous Driving Behavior Using Car-Following Data. Transportation Research Record. 1852. 10.3141/1852-18.

SAE, 2018. J3016. https://www.sae.org/news/press-room/2018/12/sae-international-releases-updated-visual-chart-for-its-%E2%80%9Clevels-of-driving-automation%E2%80%9D-standard-for-self-driving-vehicles

S. Thrun, M. Montemerlo, H. Dahlkamp, D. Stavens, A. Aron, J. Diebel, P. Fong, J. Gale,M. Halpenny, G. Ho_mann et al., 2006. Stanley: The robot that won the darpa grand challenge,"Journal of field Robotics, vol. 23, no. 9, pp. 661-692.

Scriven, M., 1967. The methodology of evaluation. In R. W. Tyler, R. M. Gagné & M.Scriven (Eds.), *Perspectives of curriculum evaluation* (Vol. 1, pp. 39-83). Chicago, IL:Rand McNally.

SemiFOT,2009. Sweden-Michigan Naturalistic Field Operational Test- https://www.saferresearch.com/library/sweden-michigan-naturalistic-field-operational-test-semifot-phase-1-final-report

Stählin, U. & Schorn, M. & Isermann, R., 2006. Avoiding emergencies by a driving assistance system for accident avoidance. 197-206.

Treat J., Tumbas N., McDonald S., Shinar D., Hume R., Mayer R., Stanisfer R., Castellan N. , 1977. Tri-level study of the causes of traffic accidents. *Report No. DOT-HS-034-3-535-77 (TAC)*.

W. Hugemann and M. Nicke, 2003. “Longitudinal and lateral accelerations in normal day driving,” in *Proceedings of the Institute of Traffic Accident Investigators Conference (ITAI ’03)*, E. J. Allen,Ed., pp. 1–8, Croydon, UK.

W. Yao, H. Zhao, P. Bonnifait, and H. Zha, 2013. "Lane change trajectory prediction by using recorded human driving data," in Intelligent Vehicles Symposium (IV), 2013 IEEE. IEEE, pp. 430–436.